

c. 3

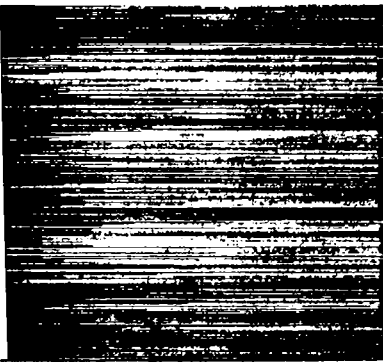
CIC-14 REPORT COLLECTION  
**REPRODUCTION  
COPY**

*ENDF/B-VI Data for MCNP™*

LOS ALAMOS NATIONAL LABORATORY



3 9338 00287 1258



**Los Alamos**  
NATIONAL LABORATORY

*Los Alamos National Laboratory is operated by the University of California  
for the United States Department of Energy under contract W-7405-ENG-36.*

*Edited by Patricia W. Mendius, Group CIC-1  
Prepared by Irene Gallegos, Group X-6*

*An Affirmative Action/Equal Opportunity Employer*

*This report was prepared as an account of work sponsored by an agency of the United States Government. Neither The Regents of the University of California, the United States Government nor any agency thereof, nor any of their employees, makes any warranty, express or implied, or assumes any legal liability or responsibility for the accuracy, completeness, or usefulness of any information, apparatus, product, or process disclosed, or represents that its use would not infringe privately owned rights. Reference herein to any specific commercial product, process, or service by trade name, trademark, manufacturer, or otherwise, does not necessarily constitute or imply its endorsement, recommendation, or favoring by The Regents of the University of California, the United States Government, or any agency thereof. The views and opinions of authors expressed herein do not necessarily state or reflect those of The Regents of the University of California, the United States Government, or any agency thereof.*

*ENDF/B-VI Data for MCNP™*

*John S. Hendricks  
Stephanie C. Frankle  
John D. Court*

LOS ALAMOS NATL. LAB. LIBS.



3 9338 00287 1258



**Los Alamos**  
NATIONAL LABORATORY

Los Alamos, New Mexico 87545

## **ERRATA**

**LA--12887:** MCNP™ ENDF/B-VI Validation  
Infinite Media Comparisons of ENDF/B-VI and ENDF/B-V

and

**LA--12891:** ENDF/B-VI Data for MCNP

**{ CORRECTIONS ARE INDICATED BY A \* }**

**Table 1.** The MCNP ENDF60 Library

Material	ZAID	Filename	Evaluation	Release	Type	Photon
<sup>1</sup> H	1001.60c	h1001	LANL	6.1 <sup>a</sup>	New <sup>b</sup>	Yes <sup>c</sup>
<sup>2</sup> H	1002.60c	d1002	LANL, AWRE	-	New	-
<sup>3</sup> H	1003.60c	t1003	LANL	-	-	No
<sup>3</sup> He	2003.60c	he2003	LANL	6.1	New	No
<sup>4</sup> He	2004.60c	he2004	LANL	-	-	No
<sup>6</sup> Li	3006.60c	li3006	LANL	6.1	New	-
<sup>7</sup> Li	3007.60c	li3007	LANL	-	New	-
<sup>9</sup> Be	4009.60c	be4009	LLNL	-	New	-
<sup>10</sup> B	5010.60c	b5010	LANL	6.1	New	-
<sup>11</sup> B	5011.60c	b5011	LANL	-	New	-
C	6000.60c	c6000	ORNL	6.1	New	-
<sup>14</sup> N	7014.60c	n7014	LANL	LANL	New	-
<sup>15</sup> N	7015.60c	n7015	LANL	-	New	-
<sup>16</sup> O	8016.60c	o8016	LANL	-	New	-
<sup>17</sup> O	8017.60c	o8017	BNL	-	-	No
<sup>19</sup> F	9019.60c	f9019	ORNL	-	New	-
<sup>23</sup> Na	11023.60c	na11023	ORNL	6.1	-	-
Mg	12000.60c	mg12000	ORNL	-	-	-
<sup>27</sup> Al	13027.60c	al13027	LANL	-	-	-
Si	14000.60c	si14000	ORNL	-	-	-
<sup>31</sup> P	15031.60c	p15031	LLNL	-	-	-
S	16000.60c	s16000	BNL	-	-	-
<sup>32</sup> S	16032.60c	s16032	LLNL	-	-	-
Cl	17000.60c	cl17000	GGA	-	-	-
K	19000.60c	k19000	GGA	-	-	-
Ca	20000.60c	ca20000	ORNL	-	New*	-
<sup>45</sup> Sc	21045.60c	sc21045	BNL	6.2	New*	-
Ti	22000.60c	ti22000	BRC, ANL	-	-	-
V	23000.60c	v23000	ANL, LLNL, +	-	New	-
<sup>50</sup> Cr	24050.60c	cr24050	ORNL	6.1	New	-

<sup>a</sup> All releases are release 6.0 of ENDF/B-VI unless otherwise noted. LANL indicates modifications were performed.

<sup>b</sup> All types are translations from ENDF/B-V Release 0, unless otherwise noted.

<sup>c</sup> All nuclides have photon production, unless otherwise noted.

**Table 1 (cont.)** The MCNP ENDF60 Library

Material	ZAID	Filename	Evaluation	Release	Type	Photon
<sup>52</sup> Cr	24052.60c	cr24052	ORNL	6.1	New	-
<sup>53</sup> Cr	24053.60c	cr24053	ORNL	6.1	New	-
<sup>54</sup> Cr	24054.60c	cr24054	ORNL	6.1	New	-
<sup>55</sup> Mn	25055.60c	mn25055	ORNL	-	New	-
<sup>54</sup> Fe	26054.60c	fe26054	ORNL	6.1	New	-
<sup>56</sup> Fe	26056.60c	fe26056	ORNL	6.1	New	-
<sup>57</sup> Fe	26057.60c	fe26057	ORNL	6.1	New	-
<sup>58</sup> Fe	26058.60c	fe26058	ORNL	6.1	New	-
<sup>59</sup> Co	27059.60c	co27059	ANL	6.2	New	-
<sup>58</sup> Ni	28058.60c	ni28058	ORNL	6.1	New	-
<sup>60</sup> Ni	28060.60c	ni28060	ORNL	6.1	New	-
<sup>61</sup> Ni	28061.60c	ni28061	ORNL	6.1	New	-
<sup>62</sup> Ni	28062.60c	ni28062	ORNL	6.1	New	-
<sup>64</sup> Ni	28064.60c	ni28062	ORNL	6.1	New	-
<sup>63</sup> Cu	29063.60c	cu29063	ORNL	6.2	New	-
<sup>65</sup> Cu	29065.60c	cu29065	ORNL	6.2	New	-
Ga	31000.60c	ga31000	LLNL, LANL	-	-	-
<sup>89</sup> Y	39089.60c	y39089	ANL, LLNL	-	New*	-
Zr	40000.60c	zr40000	SAI, BNL	6.1	-	No
<sup>93</sup> Nb	41093.60c	nb41093	ANL, LLNL	6.1	New	-
Mo	42000.60c	mo42000	LLNL, HEDL	-	-	-
<sup>99</sup> Tc	43099.60c	tc43099	HEDL, BAW	-	-	No
<sup>107</sup> Ag	47107.60c	ag47107	BNL, HEDL	-	New*	No
<sup>109</sup> Ag	47109.60c	ag47109	BNL, HEDL	-	New*	No
In	49000.60c	in49000	ANL	-	New	-
<sup>127</sup> I	53127.60c	i53127	HEDL, RCN	LANL	New*	-
<sup>129</sup> I	53129.60c	i53129	HEDL, RCN	-	-	No
<sup>133</sup> Cs	55133.60c	cs55133	HEDL, BNL, +	-	-	No
<sup>134</sup> Cs	55134.60c	cs55134	ORNL, HEDL	-	New	No
<sup>135</sup> Cs	55135.60c	cs55135	HEDL	-	-	No
<sup>136</sup> Cs	55136.60c	cs55136	HEDL	-	-	No
<sup>137</sup> Cs	55137.60c	cs55137	HEDL	-	-	No

<sup>a</sup> All releases are release 6.0 of ENDF/B-VI unless otherwise noted. LANL indicates modifications were performed.

<sup>b</sup> All types are translations from ENDF/B-V Release 0, unless otherwise noted.

<sup>c</sup> All nuclides have photon production, unless otherwise noted.

**Table 1 (cont.)** The MCNP ENDF60 Library

Material	ZAID	Filename	Evaluation	Release	Type	Photon
<sup>138</sup> Ba	56138.60c	ba56138	ORNL, HEDL	-	-	-
<sup>151</sup> Eu	63151.60c	eu63151	LANL	-	New	-
<sup>153</sup> Eu	63153.60c	eu63153	LANL	-	New	-
<sup>152</sup> Gd	64152.60c	gd64152	BNL	-	-	No
<sup>154</sup> Gd	64154.60c	gd64154	BNL	-	-	No
<sup>155</sup> Gd	64155.60c	gd64155	BNL	-	-	No
<sup>156</sup> Gd	64156.60c	gd64156	BNL	-	-	No
<sup>157</sup> Gd	64157.60c	gd64157	BNL	-	-	No
<sup>158</sup> Gd	64158.60c	gd64158	BNL	-	-	No
<sup>160</sup> Gd	64160.60c	gd64160	BNL	-	-	No
<sup>165</sup> Ho	67165.60c	ho67165	LANL	-	New	-
Hf	72000.60c	hf72000	SAI	-	-	No
<sup>181</sup> Ta	73181.60c	ta73181	LLNL	-	-	-
<sup>182</sup> Ta	73182.60c	ta73182	AI	-	-	No
<sup>182</sup> W	74182.60c	w74182	LANL, ANL, +	-	New*	-
<sup>183</sup> W	74183.60c	w74183	LANL, ANL, +	-	New*	-
<sup>184</sup> W	74184.60c	w74184	LANL, ANL, +	-	New*	-
<sup>186</sup> W	74186.60c	w74186	LANL, ANL, +	-	New*	-
<sup>185</sup> Re	75185.60c	re75185	ORNL, LANL	-	New	No
<sup>187</sup> Re	75187.60c	re75187	ORNL, LANL	-	New	No
<sup>197</sup> Au	79197.60c	au79197	LANL	6.1	New	-
<sup>206</sup> Pb	82206.60c	pb82206	ORNL	-	New	-
<sup>207</sup> Pb	82207.60c	pb82207	ORNL	6.1	New	-
<sup>208</sup> Pb	82208.60c	pb82208	ORNL	-	New	-
<sup>209</sup> Bi	83209.60c	bi83209	ANL	-	New	-
<sup>230</sup> Th	90230.60c	th90230	HEDL	-	-	No
<sup>232</sup> Th	90232.60c	th90232	BNL, ANL, +	-	-	-
<sup>231</sup> Pa	91231.60c	pa91231	HEDL	-	-	No
<sup>232</sup> U	92232.60c	u92232	HEDL	-	-	No
<sup>233</sup> U	92233.60c	u92233	LANL, ORNL	-	-	-
<sup>234</sup> U	92234.60c	u92234	BNL, GGA	-	-	No

- <sup>a</sup> All releases are release 6.0 of ENDF/B-VI unless otherwise noted. LANL indicates modifications were performed.
- <sup>b</sup> All types are translations from ENDF/B-V Release 0, unless otherwise noted.
- <sup>c</sup> All nuclides have photon production, unless otherwise noted.

**Table 1 (cont.)** The MCNP ENDF60 Library

Material	ZAID	Filename	Evaluation	Release	Type	Photon
<sup>235</sup> U	92235.60c	u92235	ORNL, LANL	6.2*	New	-
<sup>236</sup> U	92236.60c	u92236	HEDL	-	New	No
<sup>238</sup> U	92238.60c	u92238	ORNL, LANL, +	6.2	New	-
<sup>237</sup> Np	93237.60c	np93237	LANL	6.1	New	-
<sup>238</sup> Np <sup>d</sup>	93238.60c	np93238	SRL	6.2*	New	No
<sup>239</sup> Np	93239.60c	np93239	ORNL	-	New	No
<sup>236</sup> Pu	94236.60c	pu94236	HEDL, SRL	-	-*	No
<sup>237</sup> Pu	94237.60c	pu94237	HEDL	-	-*	No
<sup>238</sup> Pu	94238.60c	pu94238	HEDL, AI, +	-	-	No
<sup>239</sup> Pu	94239.60c	pu94239	LANL	6.2	New	-
<sup>240</sup> Pu	94240.60c	pu94240	ORNL	6.2*	New	-
<sup>241</sup> Pu	94241.60c	pu94241	ORNL	6.1	New	-
<sup>242</sup> Pu	94242.60c	pu94242	HEDL, SRL, +	-	-	-
<sup>243</sup> Pu	94243.60c	pu94243	BNL, SRL, +	6.2*	-	-
<sup>244</sup> Pu	94244.60c	pu94244	HEDL, SRL	-	-	No
<sup>241</sup> Am	95241.60c	am95241	CNDC	LANL	New	-
<sup>242</sup> Am <sup>d</sup>	95242.60c	am95242	SRL	6.1	-	No
<sup>243</sup> Am	95243.60c	am95243	ORNL, HEDL, +	-	New	-
<sup>241</sup> Cm	96241.60c	cm96241	HEDL	-	-	No
<sup>242</sup> Cm	96242.60c	cm96242	HEDL, SRL, +	-	-	-
<sup>243</sup> Cm	96243.60c	cm96243	HEDL, SRL, +	-	-	-
<sup>244</sup> Cm	96244.60c	cm96244	HEDL, SRL, +	-	-	-
<sup>245</sup> Cm	96245.60c	cm96245	SRL, LLNL	6.2	-	-
<sup>246</sup> Cm	96246.60c	cm96246	BNL, SRL, +	6.2	-	-
<sup>247</sup> Cm	96247.60c	cm96247	BNL, SRL, +	6.2	-	-
<sup>248</sup> Cm	96248.60c	cm96248	HEDL, SRL, +	-	-	-
<sup>249</sup> Bk	97249.60c	bk97249	CNDC	-	New	No
<sup>249</sup> Cf	98249.60c	cf98249	CNDC	LANL	New	No
<sup>250</sup> Cf	98250.60c	cf98250	BNL, SRL, +	6.2	-	-
<sup>251</sup> Cf	98251.60c	cf98251	BNL, SRL, +	6.2	-	-
<sup>252</sup> Cf	98252.60c	cf98252	BNL, SRL, +	6.2*	-	-

- <sup>a</sup> All releases are release 6.0 of ENDF/B-VI unless otherwise noted. LANL indicates modifications were performed.
- <sup>b</sup> All types are translations from ENDF/B-V Release 0, unless otherwise noted.
- <sup>c</sup> All nuclides have photon production, unless otherwise noted.
- <sup>d</sup> These data files are not recommended for use due to the evaluations being incomplete, and are currently being removed from distribution. Additionally, 95242.60c represents the ground state of <sup>242</sup>Am, not the metastable state.

# ENDF/B-VI Data for MCNP™

by

John S. Hendricks, Stephanie C. Frankle and John D. Court

## ABSTRACT

Nuclear and atomic data are the foundation upon which the radiation transport codes are built. For neutron transport the international standard is the Evaluated Nuclear Data File from Brookhaven National Laboratory. The latest version, ENDF/B-VI release 2, has recently become available for use in the Monte Carlo N-Particle (MCNP) radiation transport code. These neutron cross-section data are designated by ZAID identifiers ending in .60c and are referred to as the ENDF60 library. The ENDF60 data library was processed from the ENDF/B-VI evaluations using the NJOY code. Fifty-two percent of the data evaluations are translations from ENDF/B-V. The remaining 48% are new evaluations which have sometimes changed significantly. The RSIC release package contains the ENDF60 neutron library, a new photon library MCPLIB02, the electron library EL1, and an updated XSDIR file. We report here the work done by the LANL Radiation Transport Group (X-6) in testing and validating the ENDF60 data library and in developing the necessary new sampling and detector schemes. When the ENDF60 library should be used in preference to the previous libraries, is also considered. The development of the new photon library MCPLIB02 is also discussed.

---

MCNP is a trademark of the Regents of the University of California, Los Alamos National Laboratory.

## I. INTRODUCTION

We report here for the first time the availability of an "official" set of ENDF/B-VI neutron data for MCNP<sup>TM</sup>. ENDF/B-VI neutron data have been available for about four years, with Release 2 available in June of 1993. However, these data were not available to MCNP until MCNP4A<sup>1</sup> was released October 1, 1993, because MCNP did not have the necessary sampling schemes for new ENDF/B-VI representations of angular scattering. The new ENDF/B-VI neutron cross section data processed for MCNP are designated by Z Aid identifiers ending in .60c and are referred to as the ENDF60 library. The ENDF60 data library was processed from the ENDF/B-VI files using the NJOY code under the direction of the Nuclear Theory and Applications group (T-2) at LANL.

Fifty-two percent of the ENDF/B-VI data are translated evaluations from ENDF/B-V for which there should be only slight differences due to processing. The remaining 48% are new evaluations which have sometimes changed significantly. Each data file is referenced by a file name of the format EEZZAAA, where EE is the elemental symbol, ZZ is the atomic number, and AAA is the isotope or 000 indicating a natural element file. Table 1 describes the individual data files of the ENDF60 library. The Z Aid, file name, evaluation group, evaluation type, revision number, and photon production availability are given for each nuclide. The evaluation group is identified by the laboratory participants who performed the evaluation, and the evaluation type indicates whether the ENDF/B-VI evaluation is a new evaluation (New) or is a translation of the ENDF/B-V evaluation. If the data file is a new evaluation, the corresponding revision number for the ENDF/B-VI release is specified, where - indicates release 6.0 and may correspond to a new or translated evaluation. If the evaluation has been modified at Los Alamos, to add in photon production for instance, the revision number has been specified as LANL.

The LANL Radiation Transport Group (X-6) has developed sampling schemes for the new ENDF/B-VI data for both forward transport and next-event estimator detector schemes. These new laws are described in Section II. Section III describes why an official ENDF60 library was released. Section IV describes the photon library which is distributed along with the ENDF60 library. Sections V-IX describe the testing phase of the ENDF60 library which includes the infinite medium tests, photon production assessment, Livermore pulsed sphere benchmarks, and iron benchmarks. These tests are all described here, but are described in further detail in companion LA reports. Section X describes the criticality tests performed, and this report is the only publication of these results. Section XI describes the changes required in the original NJOY produced data as a result of the testing, and Section XII describes the approximations made by NJOY for the Oak Ridge National Laboratory (ORNL) evaluations in detail. The ENDF60 library package was released for international distribution to the Radiation Shielding

Table 1: The MCNP ENDF60 Library.

Material	ZAID	Filename	Evaluation	Revision	Type	Photon
<sup>1</sup> H	1001.60c	h1001	LANL	<sup>a</sup> 6.1	<sup>b</sup> New	<sup>c</sup> Yes
<sup>2</sup> H	1002.60c	d1002	LANL, AWRE	-	New	-
<sup>3</sup> H	1003.60c	t1003	LANL	-	-	No
<sup>3</sup> He	2003.60c	he2003	LANL	6.1	New	No
<sup>4</sup> He	2004.60c	he2004	LANL	-	-	No
<sup>6</sup> Li	3006.60c	li3006	LANL	6.1	New	-
<sup>7</sup> Li	3007.60c	li3007	LANL	-	New	-
<sup>9</sup> Be	4009.60c	be4009	LLNL	-	New	-
<sup>10</sup> B	5010.60c	b5010	LANL	6.1	New	-
<sup>11</sup> B	5011.60c	b5011	LANL	-	New	-
C	6000.60c	c6000	ORNL	6.1	New	-
<sup>14</sup> N	7014.60c	n7014	LANL	LANL	New	-
<sup>15</sup> N	7015.60c	n7015	LANL	-	New	-
<sup>16</sup> O	8016.60c	o8016	LANL	-	New	-
<sup>17</sup> O	8017.60c	o8017	BNL	-	-	No
<sup>19</sup> F	9019.60c	f9019	ORNL	-	New	-
<sup>23</sup> Na	11023.60c	na11023	ORNL	6.1	-	-
Mg	12000.60c	mg12000	ORNL	-	-	-
<sup>27</sup> Al	13027.60c	al13027	LANL	-	-	-
Si	14000.60c	si14000	ORNL	-	-	-
<sup>31</sup> P	15031.60c	p15031	LLNL	-	-	-
S	16000.60c	s16000	BNL	-	-	-
<sup>32</sup> S	16032.60c	s16032	LLNL	-	-	-
Cl	17000.60c	cl17000	GGA	-	-	-
K	19000.60c	k19000	GGA	-	-	-
Ca	20000.60c	ca20000	ORNL	-	-	-
<sup>45</sup> Sc	21045.60c	sc21045	BNL	6.2	-	-
Ti	22000.60c	ti22000	BRC, ANL	-	-	-
V	23000.60c	v23000	ANL, LLNL, +	-	New	-
<sup>50</sup> Cr	24050.60c	cr24050	ORNL	6.1	New	-

<sup>a</sup>All revisions are revision 6.0 of ENDF/B-VI unless otherwise noted. LANL indicates modifications were performed.

<sup>b</sup>All types are translations from ENDF/B-V, unless otherwise noted.

<sup>c</sup>All nuclides have photon production, unless otherwise noted.

Table 1 (cont.) The MCNP ENDF60 Library.

Material	ZAID	Filename	Evaluation	Revision	Type	Photon
<sup>52</sup> Cr	24052.60c	cr24052	ORNL	6.1	New	-
<sup>53</sup> Cr	24053.60c	cr24053	ORNL	6.1	New	-
<sup>54</sup> Cr	24054.60c	cr24054	ORNL	6.1	New	-
<sup>55</sup> Mn	25055.60c	mn25055	ORNL	-	New	-
<sup>54</sup> Fe	26054.60c	fe26054	ORNL	6.1	New	-
<sup>56</sup> Fe	26056.60c	fe26056	ORNL	6.1	New	-
<sup>57</sup> Fe	26057.60c	fe26057	ORNL	6.1	New	-
<sup>58</sup> Fe	26058.60c	fe26058	ORNL	6.1	New	-
<sup>59</sup> Co	27059.60c	co27059	ANL	6.2	New	-
<sup>58</sup> Ni	28058.60c	ni28058	ORNL	6.1	New	-
<sup>60</sup> Ni	28060.60c	ni28060	ORNL	6.1	New	-
<sup>61</sup> Ni	28061.60c	ni28061	ORNL	6.1	New	-
<sup>62</sup> Ni	28062.60c	ni28062	ORNL	6.1	New	-
<sup>64</sup> Ni	28064.60c	ni28062	ORNL	6.1	New	-
<sup>63</sup> Cu	29063.60c	cu29063	ORNL	6.2	New	-
<sup>65</sup> Cu	29065.60c	cu29065	ORNL	6.2	New	-
Ga	31000.60c	ga31000	LLNL, LANL	-	-	-
<sup>89</sup> Y	39089.60c	y39089	ANL, LLNL	-	-	-
Zr	40000.60c	zr40000	SAI, BNL	6.1	-	No
<sup>93</sup> Nb	41093.60c	nb41093	ANL, LLNL	6.1	New	-
Mo	42000.60c	mo42000	LLNL, HEDL	-	-	-
<sup>99</sup> Tc	43099.60c	tc43099	HEDL, BAW	-	-	No
<sup>107</sup> Ag	47107.60c	ag47107	BNL, HEDL	-	-	No
<sup>109</sup> Ag	47109.60c	ag47109	BNL, HEDL	-	-	No
In	49000.60c	in49000	ANL	-	New	-
<sup>127</sup> I	53127.60c	i53127	HEDL, RCN	LANL	-	-
<sup>129</sup> I	53129.60c	i53129	HEDL, RCN	-	-	No
<sup>133</sup> Cs	55133.60c	cs55133	HEDL, BNL, +	-	-	No
<sup>134</sup> Cs	55134.60c	cs55134	ORNL, HEDL	-	New	No
<sup>135</sup> Cs	55135.60c	cs55135	HEDL	-	-	No
<sup>136</sup> Cs	55136.60c	cs55136	HEDL	-	-	No
<sup>137</sup> Cs	55137.60c	cs55137	HEDL	-	-	No

All revisions are revision 6.0 of ENDF/B-VI unless otherwise noted. LANL indicates modifications were performed.

All types are translations from ENDF/B-V, unless otherwise noted.

All nuclides have photon production, unless otherwise noted.

Table 1 (cont.) The MCNP ENDF60 Library.

Material	ZAID	Filename	Evaluation	Revision	Type	Photon
<sup>138</sup> Ba	56138.60c	ba56138	ORNL, HEDL	-	-	-
<sup>151</sup> Eu	63151.60c	eu63151	LANL	-	New	-
<sup>153</sup> Eu	63153.60c	eu63153	LANL	-	New	-
<sup>152</sup> Gd	64152.60c	gd64152	BNL	-	-	No
<sup>154</sup> Gd	64154.60c	gd64154	BNL	-	-	No
<sup>155</sup> Gd	64155.60c	gd64155	BNL	-	-	No
<sup>156</sup> Gd	64156.60c	gd64156	BNL	-	-	No
<sup>157</sup> Gd	64157.60c	gd64157	BNL	-	-	No
<sup>158</sup> Gd	64158.60c	gd64158	BNL	-	-	No
<sup>160</sup> Gd	64160.60c	gd64160	BNL	-	-	No
<sup>165</sup> Ho	67165.60c	ho67165	LANL	-	New	-
Hf	72000.60c	hf72000	SAI	-	-	No
<sup>181</sup> Ta	73181.60c	ta73181	LLNL	-	-	-
<sup>182</sup> Ta	73182.60c	ta73182	AI	-	-	No
<sup>182</sup> W	74182.60c	w74182	LANL, ANL, +	-	-	-
<sup>183</sup> W	74183.60c	w74183	LANL, ANL, +	-	-	-
<sup>184</sup> W	74184.60c	w74184	LANL, ANL, +	-	-	-
<sup>186</sup> W	74186.60c	w74186	LANL, ANL, +	-	-	-
<sup>185</sup> Re	75185.60c	re75185	ORNL, LANL	-	New	No
<sup>187</sup> Re	75187.60c	re75187	ORNL, LANL	-	New	No
<sup>197</sup> Au	79197.60c	au79197	LANL	6.1	New	-
<sup>206</sup> Pb	82206.60c	pb82206	ORNL	-	New	-
<sup>207</sup> Pb	82207.60c	pb82207	ORNL	6.1	New	-
<sup>208</sup> Pb	82208.60c	pb82208	ORNL	-	New	-
<sup>209</sup> Bi	83209.60c	bi83209	ANL	-	New	-
<sup>230</sup> Th	90230.60c	th90230	HEDL	-	-	No
<sup>232</sup> Th	90232.60c	th90232	BNL, ANL, +	-	-	-
<sup>231</sup> Pa	91231.60c	pa91231	HEDL	-	-	No
<sup>232</sup> U	92232.60c	u92232	HEDL	-	-	No
<sup>233</sup> U	92233.60c	u92233	LANL, ORNL	-	-	-
<sup>234</sup> U	92234.60c	u92234	BNL, GGA	-	-	No

All revisions are revision 6.0 of ENDF/B-VI unless otherwise noted. LANL indicates modifications were performed.

All types are translations from ENDF/B-V, unless otherwise noted.

All nuclides have photon production, unless otherwise noted.

Table 1 (cont.) The MCNP ENDF60 Library.

Material	ZAID	Filename	Evaluation	Revision	Type	Photon
<sup>235</sup> U	92235.60c	u92235	ORNL, LANL	LANL	New	-
<sup>236</sup> U	92236.60c	u92236	HEDL	-	New	No
<sup>238</sup> U	92238.60c	u92238	ORNL, LANL, +	6.2	New	-
<sup>237</sup> Np	93237.60c	np93237	LANL	6.1	New	-
<sup>238</sup> Np	93238.60c	np93238	SRL	LANL	New	No
<sup>239</sup> Np	93239.60c	np93239	ORNL	-	New	No
<sup>236</sup> Pu	94236.60c	pu94236	HEDL, SRL	-	New	No
<sup>237</sup> Pu	94237.60c	pu94237	HEDL	-	New	No
<sup>238</sup> Pu	94238.60c	pu94238	HEDL, AI, +	-	-	No
<sup>239</sup> Pu	94239.60c	pu94239	LANL	6.2	New	-
<sup>240</sup> Pu	94240.60c	pu94240	ORNL	LANL	New	-
<sup>241</sup> Pu	94241.60c	pu94241	ORNL	6.1	New	-
<sup>242</sup> Pu	94242.60c	pu94242	HEDL, SRL, +	-	-	-
<sup>243</sup> Pu	94243.60c	pu94243	BNL, SRL, +	LANL	-	-
<sup>244</sup> Pu	94244.60c	pu94244	HEDL, SRL	-	-	No
<sup>241</sup> Am	95241.60c	am95241	CNDC	LANL	New	-
<sup>242</sup> Am	95242.60c	am95242	SRL	6.1	-	No
<sup>243</sup> Am	95243.60c	am95243	ORNL, HEDL, +	-	New	-
<sup>241</sup> Cm	96241.60c	cm96241	HEDL	-	-	No
<sup>242</sup> Cm	96242.60c	cm96242	HEDL, SRL, +	-	-	-
<sup>243</sup> Cm	96243.60c	cm96243	HEDL, SRL, +	-	-	-
<sup>244</sup> Cm	96244.60c	cm96244	HEDL, SRL, +	-	-	-
<sup>245</sup> Cm	96245.60c	cm96245	SRL, LLNL	6.2	-	-
<sup>246</sup> Cm	96246.60c	cm96246	BNL, SRL, +	6.2	-	-
<sup>247</sup> Cm	96247.60c	cm96247	BNL, SRL, +	6.2	-	-
<sup>248</sup> Cm	96248.60c	cm96248	HEDL, SRL, +	-	-	-
<sup>249</sup> Bk	97249.60c	bk97249	CNDC	-	New	No
<sup>249</sup> Cf	98249.60c	cf98249	CNDC	LANL	New	No
<sup>250</sup> Cf	98250.60c	cf98250	BNL, SRL, +	6.2	-	-
<sup>251</sup> Cf	98251.60c	cf98251	BNL, SRL, +	6.2	-	-
<sup>252</sup> Cf	98252.60c	cf98252	BNL, SRL, +	LANL	-	-

All revisions are revision 6.0 of ENDF/B-VI unless otherwise noted. LANL indicates modifications were performed.

All types are translations from ENDF/B-V, unless otherwise noted.

All nuclides have photon production, unless otherwise noted.

Information Center (RSIC) in October, 1994. To obtain the library package, contact RSIC, P. O. Box 2008, Oak Ridge, Tennessee, 37831-6362, USA. Phone (615) 574-6176, Fax (615) 574-6182, E-mail: PDC@ORNL.GOV.

## II. NEW SCATTERING LAWS

MCNP4A added three new ENDF/B-VI scattering laws complete with new data formats and processing, transport physics, and next-event estimator (point detector) sampling schemes. These three laws are the Kalbach-87 formalism (ENDF/B-VI file 6 LAW=1, LANG=2), correlated angle-energy scattering (ENDF/B-VI file 6 LAW=7), and phase-space law (ENDF/B-VI file 6 LAW=6.)

The Kalbach-87 formalism, ENDF/B-VI file 6 LAW=1, LANG=2 or MCNP Law 44, requires sampling the cosine between the incident and outgoing particle directions,  $\mu$ , from the density function:

$$p(\mu, E, E') = \frac{1}{2} \frac{A}{\sinh(A)} [\cosh(A\mu) + R \sinh(A\mu)], \quad (1)$$

where  $E$  is the incident energy,  $E'$  is the exiting energy, and  $\mu$  is the cosine between the incident and outgoing particle directions. The  $R$  and  $A$  values are found from tabulated values with an  $R$  and  $A$  value for each  $E'$ , and a table of  $E'$  values for each  $E$ . The Kalbach-87 formalism is used for many of the new ENDF/B-VI evaluations, and it is also used as an approximation for the new ORNL evaluations with the exception of F.

The correlated angle-energy scattering law, ENDF/B-VI file 6 LAW=7 or MCNP Law 67, first samples  $\mu$  from 32-equiprobable cosine bins between incident and outgoing particle direction with interpolation for a given incident energy,  $E$ . Then, with  $\mu$  and  $E$  known, the outgoing energy,  $E'$ , is sampled from tables interpolated on the  $\mu$  and  $E$  tables. That is,  $\mu$  and  $E'$  are sampled from a three-dimensional table in  $E$ ,  $\mu$ , and  $E'$ , with full interpolation. This tabular correlated angle-energy scattering law is used for  ${}^9\text{Be}$  only in ENDF/B-VI. This law is also used as an approximation for the new ENDF/B-VI Legendre expansion law in the case of F only.

The correlated angle-energy scattering phase-space law, ENDF/B-VI file 6 LAW= 6 or MCNP Law 66, first samples the outgoing particle direction cosine,  $\mu$ , isotropically in the center-of-mass system. Then, given the number of bodies in phase space  $n$ , and the total mass ratio  $A_p$  for  $n$  particles,

$$E' = TE_i^{max}, \quad (2)$$

where  $T$  is sampled from the density function:

$$p(\mu, E, T) = C_n \sqrt{T} (E_i^{max} - T)^{3n/2-4}, \quad (3)$$

and where  $E_i^{max}$  is the maximum possible energy for particle  $i$ ,  $\mu$ , and  $E'$ :

$$E_i^{max} = \frac{A_p - 1}{A_p} \left( \frac{A}{A + 1} E + Q \right). \quad (4)$$

Here  $C_n$  is a normalization constant,  $A$  is the atomic weight ratio, and  $Q$  is the  $Q$ -value of the reaction. This law is used for ENDF/B-VI deuterium only with  $n = 3$ .

In addition to the algorithms to sample these laws for neutron transport, new algorithms were developed for next-event estimators so that collisions using these new laws now contribute to point and ring detectors as well as the DXTRAN variance reduction method. The NJOY code was also modified by T-2 to provide data in these new formats.

There is an additional new law in the ENDF/B-VI evaluations. The ORNL evaluators produced evaluations of F, Cr, Mn, Fe, Ni, Cu, and Pb isotopes using Legendre expansions to represent energy-angle distribution in the laboratory system. Whereas MCNP4A does not yet have a sampling scheme for this representation, NJOY reformulates these scattering distributions according to the Kalbach-87 distribution for use in MCNP for all except F which uses the correlated angle-energy law. A further discussion of these approximations to the Legendre expansion law is given in Section XII.

### III. OTHER MCNP ENDF/B-VI LIBRARIES

Since the release of NJOY91.91, dozens of ENDF/B-VI MCNP compatible data libraries have been generated around the world. These libraries have been generated with different assumptions suitable for the sites where they were produced. In particular, the continuous-energy neutron data of MCNP requires a pointwise-linear unionized grid; that is, all reaction cross sections are on the same energy grid with linear-linear interpolation. Because an infinite number of points is required to give an exact continuous-energy representation, which is impossible, the energy grid must be thinned. This thinning is accomplished by preserving the cross-section integral weighting, to some specified tolerance. For example, fusion applications would use constant weighting, whereas reactor applications would use  $1/E$  weighting. Different thinning tolerances would be used depending upon the computer storage capacities at different sites. Further, different ways of arranging the data into libraries were used. Consequently there are many MCNP compatible libraries of ENDF/B-VI data around the world and it is very confusing as to which data set is which. The MCNP developers felt there was a need for a standard, or "official", set of ENDF/B-VI data, just as there are standard sets of ENDF/B-V and other data.

To provide a standard MCNP ENDF/B-VI library, the Radiation Transport group engaged the Nuclear Theory and Applications Group to construct a complete library based on ENDF/B-VI through revision 2. This ENDF60 library contains 70 revision 0, 26 revision 1, and only 11 revision 2 data. Special modifications to 9 nuclides were made by T-2 and are indicated as

LANL in Table 1. This library was thinned such that most nuclides were no more than 400,000 words in storage length (3.2 megabytes), used flat weighting, and were at room temperature. The unique identifiers assigned to this library were .60C such that any reference to the Z Aid=ZZZAAA.60C in MCNP would denote this library and nothing else. This new library is henceforth referred to as the ENDF60 library. The ENDF60 library is stored by nuclide rather than grouped into a larger library as was done previously for RMCCS. For example, the data file h1001 is hydrogen, pu94239 is  $^{239}\text{Pu}$ , etc. This allows the user to keep only the necessary data files, thereby reducing the required storage space.

The ENDF60 library is made up of 124 nuclides in MCNP Type 1 (ascii) format, which can be used on any computer platform. It requires approximately 200 megabytes of disk space for the complete library, with an average data file size of 1.6 megabytes. The largest nuclide is  $^{127}\text{I}$  which takes 8.1 megabytes, considerably more than the 400,000 word guideline. The RSIC release package includes the ENDF60 neutron library, the new photon library MCPLIB02, the electron library EL1, and a new XSDIR file. The new photon data library MCPLIB02 extends the photon interaction data up to 100 GeV and is described in detail in the following section. As in the original MCPLIB library, MCPLIB02 only includes data for  $Z \leq 94$ . Therefore, coupled neutron-photon problems cannot be performed using ENDF60 for  $Z > 94$ . It is anticipated that a new photon library which will include  $Z \geq 95$  will be released within a year. In addition to the XSDIR entries for the new data libraries, this updated XSDIR file has been further modified such that the default data libraries are now the MCNP recommended libraries as indicated in Appendix G of the MCNP4A manual, as well as defining MCPLIB02 to be the default photon library.

#### IV. THE MCPLIB02 PHOTON LIBRARY

MCNP is unable to run coupled neutron-photon problems without photon data, and electron data for the thick target bremsstrahlung treatment in the default case. Consequently, the ENDF60 library release to RSIC includes a new photon library, MCPLIB02, and the electron library, EL1. The MCPLIB02 library consists of photon cross sections with Z Aid identifiers ending in .02P. The capability to utilize more than one evaluation of photons or electrons was added to MCNP4A using the PLIB or ELIB parameters on the materials (MAT) cards. The MCPLIB02 library is an extension of the original MCPLIB library which has been in use for over 15 years, extending the photon interaction data from 100 MeV to 100 GeV based upon the Lawrence Livermore National Laboratory (LLNL) Evaluated Photon Data Library (EPDL).

EPDL contains considerably more detail than MCNP4A is currently prepared to use. For example, the EPDL distinguishes between pair- and triplet-production cross sections, tabulates real and imaginary anomalous scattering factors, and includes photoelectric subshell cross sections for shells as high-lying as Q1. As a long-term project, it would be desirable to incorporate all of this detail into MCNP. For the first implementation of EPDL data, the energy

range for the photon interaction data was extended leaving the sampling algorithms unchanged. Specifically, EPDL data is incorporated above the maximum energy available in MCPLIB, and a smooth transition is made from MCPLIB to EPDL between these limiting energies. The maximum energy in MCPLIB is usually 100 MeV, but for seven elements ( $Z = 84, 85, 87, 88, 89, 91,$  and  $93$ ) it is 15 MeV. For each element, five blocks of MCPLIB data have been extended. These are the incoherent, coherent, photoelectric, and pair production cross sections, and the heating numbers. The remaining blocks of data (incoherent, coherent, and integrated coherent form factors, and fluorescence data) remain unchanged. Since MCPLIB data are used at low energies, the new MCPLIB02 data are backward-compatible with most existing MCNP photon calculations; but high-energy applications up to the limit of the electron data (1 GeV) are now possible.

Unlike the MCPLIB data, the EPDL uses a different energy grid for tabulating each separate photon cross section. For MCPLIB02 a common grid was chosen on which to tabulate all new data above 10 MeV. This grid is based on the EPDL grid for pair production cross sections, both because the pair-production energy grid has the greatest resolution, and because pair production is the most important process at high energies. Both the EPDL and the MCPLIB cross-section data (and the MCPLIB heating numbers) rely on logarithmic interpolation to evaluate quantities at energies between tabulated points:

$$\sigma = F(E_1, E_2, \sigma_1, \sigma_2, E) = \exp \left( \frac{ \left\{ \ln \left[ \frac{E}{E_1} \right] \ln[\sigma_2] + \ln \left[ \frac{E_2}{E} \right] \ln[\sigma_1] \right\} }{ \ln \left[ \frac{E_2}{E_1} \right] } \right). \quad (5)$$

The EPDL also calls for the use of linear interpolation for certain quantities. The important quantities relying on linear interpolation are the average energies  $\Delta E$  of secondary particles.

The procedure for merging MCPLIB and EPDL data for each element into the new library was as follows. For energies between 1 keV and 10 MeV, the MCPLIB energy grid and data were included unchanged. The maximum energy  $\epsilon$  available in MCPLIB was identified. ( $\epsilon$  is either 15 MeV or 100 MeV). For energies  $E$  in the transition range  $10 \text{ MeV} < E < \epsilon$ , the MCPLIB cross section  $\sigma_E$  was determined for each process. An interpolated cross section

$$\sigma = F(10.0, \epsilon, \sigma_M, \sigma_E, E) \quad (6)$$

was used for that process in MCPLIB02. Above  $\epsilon$ , the EPDL cross section was determined, interpolating as needed, and used unchanged. Whenever a pair cross section had to be extracted from the EPDL, the sum of the pair and triplet cross sections was used, since MCPLIB does not separate the two processes.

There is no quantity comparable to the MCPLIB heating number in the EPDL, so heating numbers were constructed according to the formula

$$H(E) = \frac{\sum_i \Delta E_i(E) \sigma_i(E)}{\sigma_{total}(E)}, \quad (7)$$

where  $H(E)$  is an MCPLIB-style heating number as a function of energy  $E$ ; the summation index  $i$  labels the incoherent, photoelectric, pair, and triplet processes; and  $\Delta E_i(E)$  is the average secondary electron energy from process  $i$ , except in the case of photoelectric absorption, when  $\Delta E_i(E)$  also includes the energy of those fluorescent X-rays not explicitly accounted for in the EPDL. Since the EPDL accounts for X-rays from many more shells than does MCPLIB, Eq. 7 is not strictly consistent with the MCPLIB heating numbers. Fortunately, at the high energies above MCPLIB this inconsistency is completely negligible.

For 87 of the 94 elements in MCPLIB02, an artificial, small pair-production cross section ( $10^{-6}$  barn) is included at the pair production threshold (1.022 MeV). This prevents the MCNP interpolation scheme from returning zero for the pair-production cross section all the way up to the first real data point (1.5 MeV). The seven elements whose maximum MCPLIB energies were only 15 MeV also lacked this special starting point for the pair cross section. An energy point at 1.022 MeV for these seven elements was inserted, so that the treatment of pair production is now consistent across the entire database. Other cross sections and heating numbers at this point were derived by logarithmic interpolation, so that the sampled values for these quantities will not be affected.

## V. TESTING AND RELEASE OF THE ENDF60 LIBRARY

In order to get the ENDF60 library out in a timely fashion, the testing and validation phase was radically changed from in the past. In particular, the former manual checking used in previous libraries was not implemented. Therefore, a new set of quality assurance tests was established for NJOY and carried out by T-2. In addition to these tests, X-6 subjected the data to a number of customized checks, ENDF/B-V comparisons, and experimental benchmark comparisons. Extensive tests were carried out to ensure that the new scattering laws were properly implemented in MCNP and that both transport and next-event estimator solutions agreed.

The ENDF60 library was compared with a number of other data libraries. In particular, infinite medium simulations were performed for all nuclides in the ENDF60 data library, comparing them to the recommended data libraries from Appendix G of the MCNP4A manual, and to the ENDL-90 data library when appropriate. In general, the MCNP recommended data libraries are based on ENDF/B-V evaluations. When this is not the case, the recommended data library has often been produced by T-2 at LANL and is indicated as the T-2 recommended data library in the discussion. For nuclides where ENDF/B-V, ENDF/B-VI, and T-2 recommended

libraries are available, all three were compared. THE ENDF60 library was also benchmarked against experimental data for the 47 nuclides listed in Table 2. These experimental benchmarks consisted of the LLNL pulsed sphere experiments, a set of iron benchmark experiments, and a set of criticality experiments.

## VI. INFINITE MEDIUM TESTS

All ENDF60 nuclides were run with MCNP and compared to ENDF/B-V in infinite medium simulations. Comparisons were also made with the MCNP recommended data libraries when these were not ENDF/B-V. The infinite medium simulations consisted of a 20-MeV neutron source in an 100-m radius sphere of the nuclide. For light materials this was sufficient to downscatter throughout the entire energy range. As materials got heavier, the source was modified so that for the heaviest elements the source spanned the entire energy range so as to sample collisions for the entire energy range. The neutron flux and heating were then tallied along with the induced photon flux and heating, and coplots were made for the ENDF/B-VI, ENDF/B-V, and the T-2 recommended libraries. All these coplots are published in a LANL Report LA-12287.<sup>2</sup>

In general, these infinite medium simulations demonstrated that for most materials ENDF/B-V and ENDF/B-VI give similar results. The neutron and photon fluxes are close, indicating that there are no gross errors in the ENDF/B-VI collision processes or reaction cross sections. The ENDF/B-VI neutron heating numbers are generally better, often being extended in range. The results for an example nuclide are provided in Figures 1-4. The ENDF/B-V and ENDF/B-VI results for  $^1\text{H}$  are coplotted for the neutron flux, neutron heating, neutron-induced photon flux, and photon heating respectively. ENDF/B-V and ENDF/B-VI agree for all but the neutron heating. As shown in Figure 2, the neutron heating is higher at low energies for ENDF/B-VI because of improvements in modeling the nucleus recoil effects that have been made in the NJOY code. These improvements also appear for some translated evaluations as illustrated in Figure 5 for Mg, and they can be quite dramatic in the case of Cl and K. Figure 6 illustrates the changes in neutron heating due to modifications in the NJOY code for Cl.

In cases where there is no photon production in ENDF/B-V but it is now present in ENDF/B-VI, the heating numbers are also again lower for ENDF/B-VI as shown in Figure 7 for  $^{197}\text{Au}$ . When photon production is not present, the photon energy is deposited as heating of the material and therefore added to the neutron heating tally. Note how the T-2 MCNP recommended library agrees with the ENDF/B-IV data because it also had photon production available. In general, the infinite media simulations for the new ENDF60 library indicate that ENDF/B-VI is an improvement over ENDF/B-V.

Table 2 MCNP ENDF60 Library Experimental Benchmark Coverage.

ZAIID	Livermore Ref.[5]	Iron Ref.[7]	Critical
<sup>1</sup> H	✓	✓	✓
<sup>2</sup> H	✓		
<sup>6</sup> Li	✓	✓	
<sup>7</sup> Li	✓	✓	
<sup>9</sup> Be	✓		
<sup>10</sup> B		✓	✓
<sup>11</sup> B		✓	✓
C	✓	✓	✓
<sup>14</sup> N	✓	✓	✓
<sup>16</sup> O	✓	✓	✓
<sup>19</sup> F	✓		✓
<sup>23</sup> Na	✓	✓	✓
Mg	✓	✓	✓
<sup>27</sup> Al	✓	✓	✓
Si	✓	✓	✓
<sup>31</sup> P	✓	✓	✓
<sup>32</sup> S	✓	✓	✓
K		✓	
Ca	✓	✓	
Ti	✓		✓
<sup>50</sup> Cr	✓	✓	✓
<sup>52</sup> Cr	✓	✓	✓
<sup>53</sup> Cr	✓	✓	✓
<sup>54</sup> Cr	✓	✓	✓

Table 2 (cont) MCNP ENDF60 Library Experimental Benchmark Coverage.

ZAID	Livermore Ref.[5]	Iron Ref.[7]	Critical
<sup>55</sup> Mn	✓	✓	✓
<sup>54</sup> Fe	✓	✓	✓
<sup>56</sup> Fe	✓	✓	✓
<sup>57</sup> Fe	✓	✓	✓
<sup>58</sup> Fe	✓	✓	✓
<sup>58</sup> Ni	✓	✓	
<sup>60</sup> Ni	✓	✓	
<sup>61</sup> Ni	✓	✓	
<sup>62</sup> Ni	✓	✓	
<sup>64</sup> Ni	✓	✓	
<sup>63</sup> Cu			✓
<sup>65</sup> Cu			✓
<sup>206</sup> Pb	✓		
<sup>207</sup> Pb	✓		
<sup>208</sup> Pb	✓		
<sup>234</sup> U			✓
<sup>235</sup> U			✓
<sup>236</sup> U			✓
<sup>238</sup> U			✓
<sup>239</sup> Pu			✓
<sup>240</sup> Pu			✓
<sup>241</sup> Pu			✓
<sup>242</sup> Pu			✓

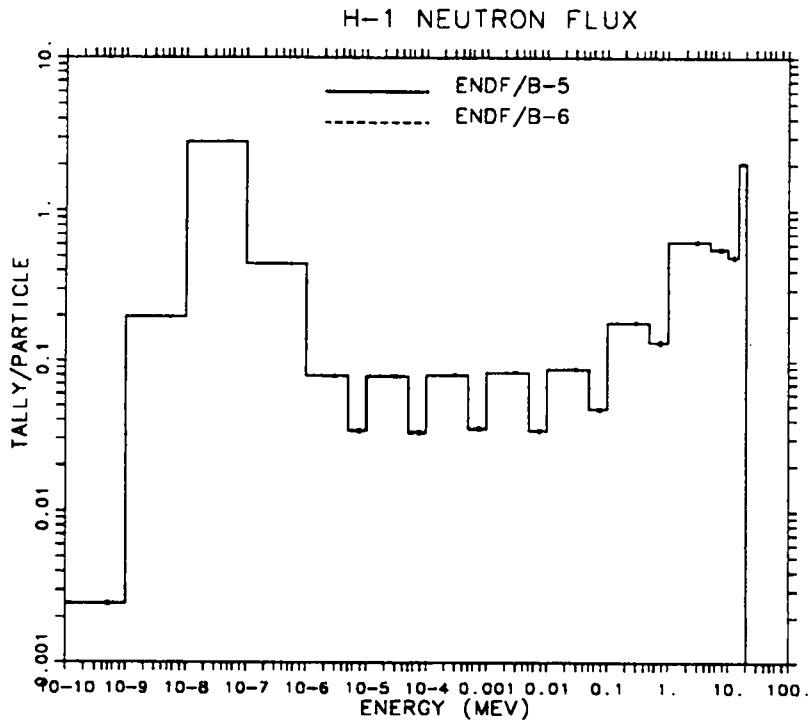


Figure 1: Plot of ENDF/B-V and ENDF/B-VI calculated neutron flux for a 10000 cm radius  $^1\text{H}$  sphere.

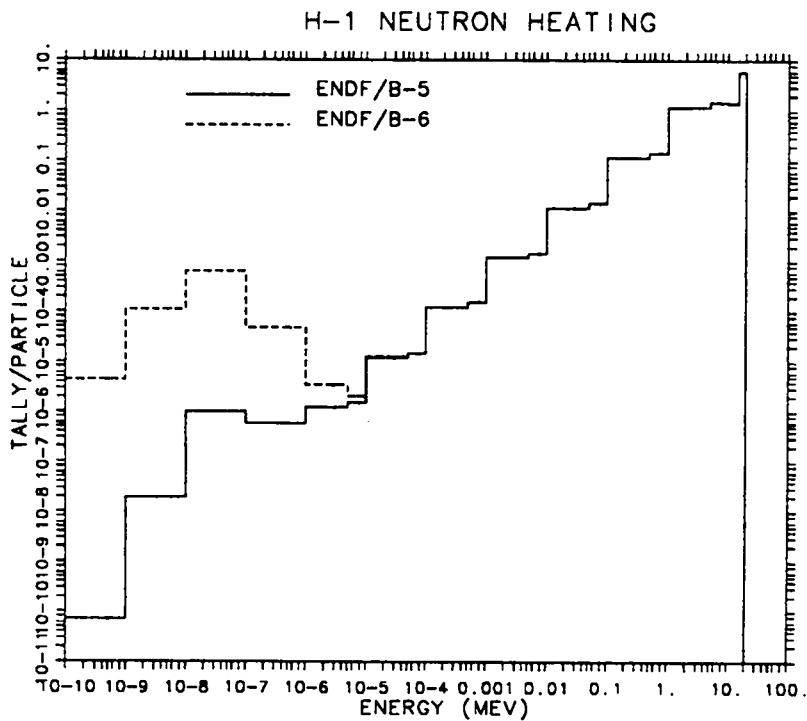


Figure 2: Plot of ENDF/B-V and ENDF/B-VI calculated neutron heating for the  $^1\text{H}$  sphere.

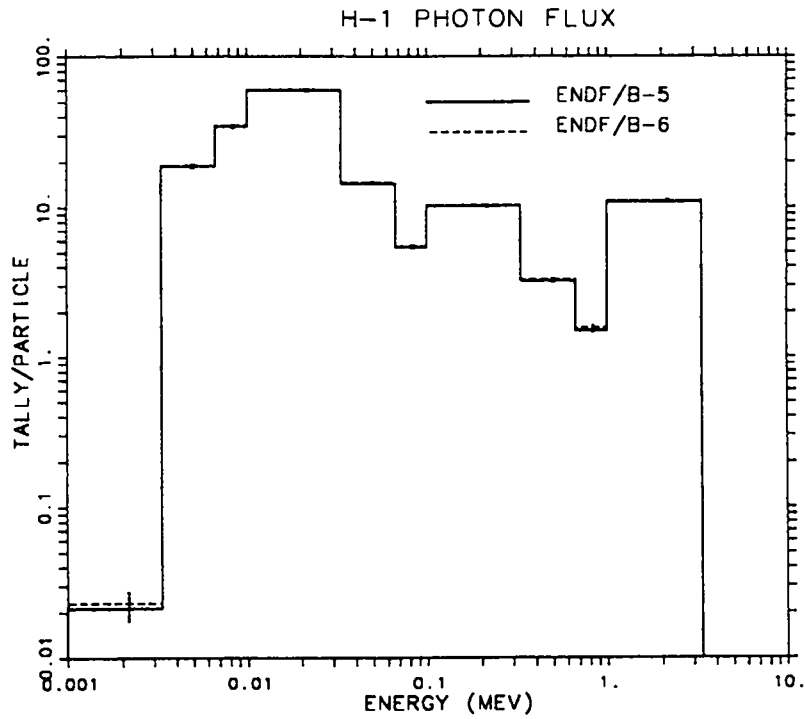


Figure 3: Plot of ENDF/B-V and ENDF/B-VI calculated photon flux for the  $^1\text{H}$  sphere.

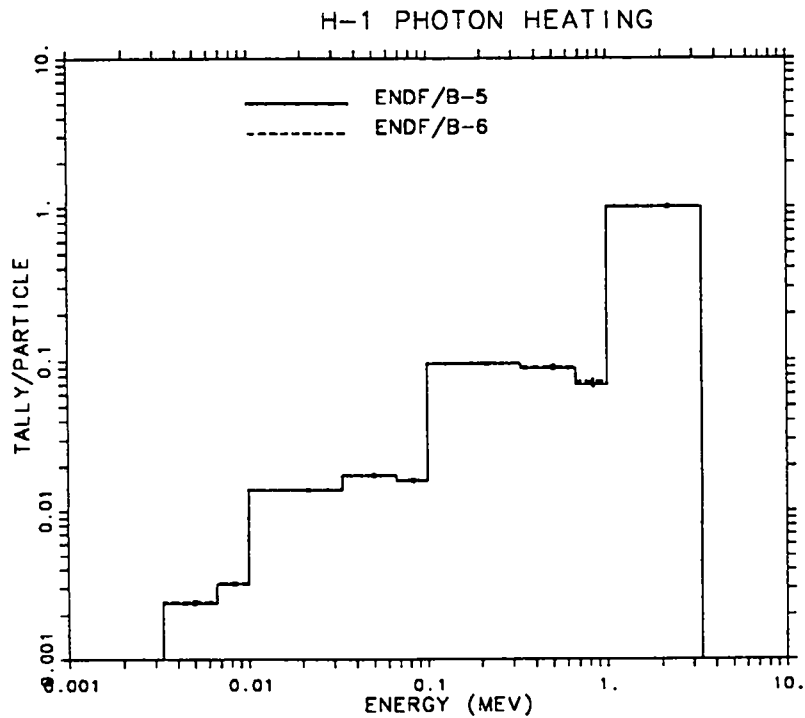


Figure 4: Plot of ENDF/B-V and ENDF/B-VI calculated photon heating for the  $^1\text{H}$  sphere.

# MG NEUTRON HEATING

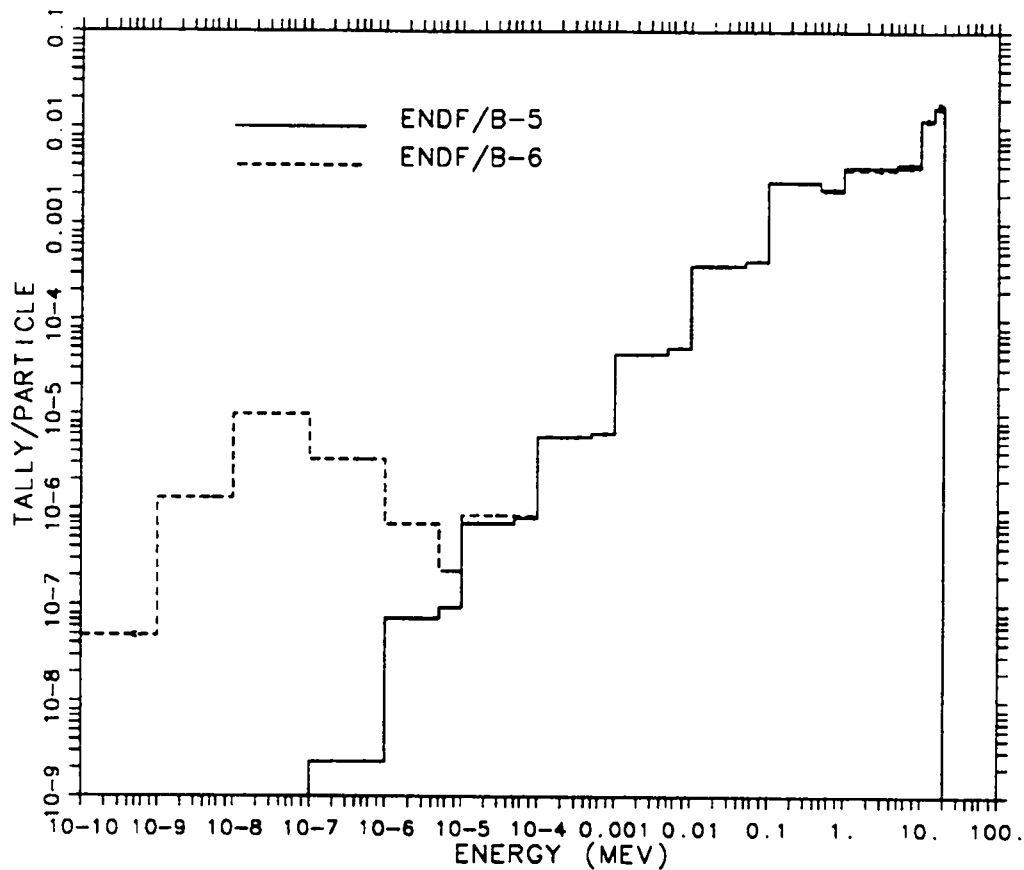


Figure 5: Plot of ENDF/B-V and ENDF/B-VI calculated neutron heating for the magnesium sphere.

# CL NEUTRON HEATING

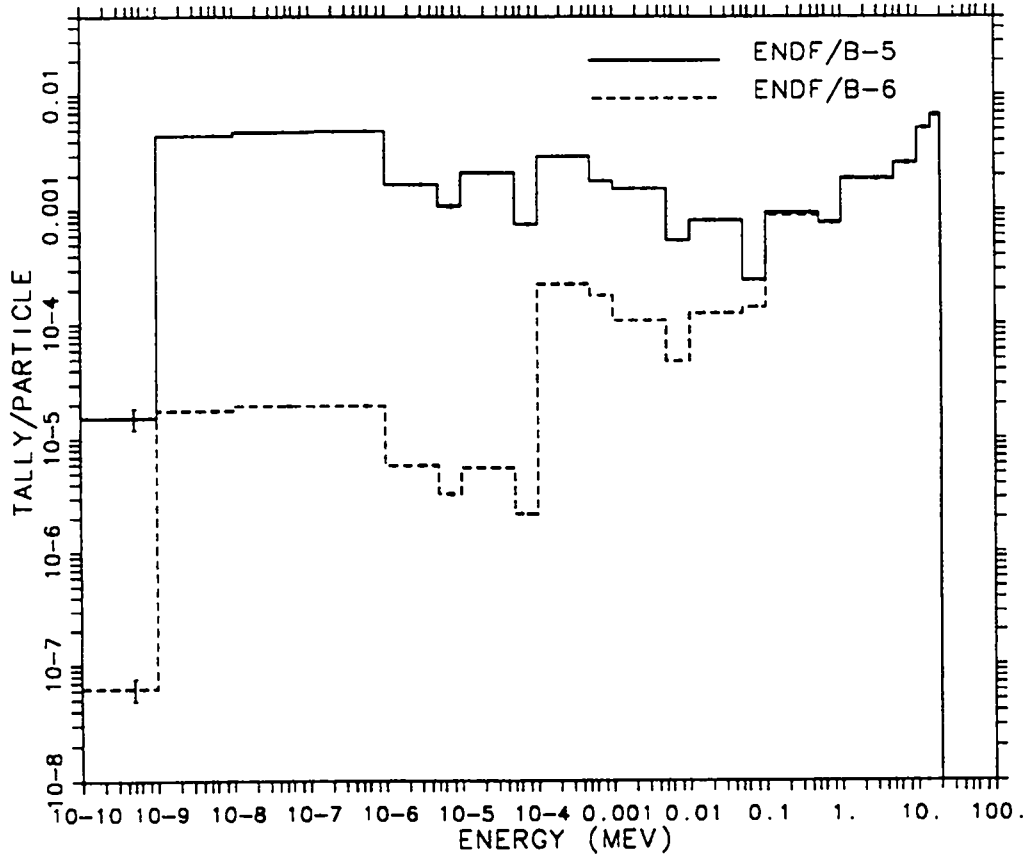


Figure 6: Plot of ENDF/B-V and ENDF/B-VI calculated neutron heating for the chlorine sphere.

# AU-197 NEUTRON HEATING

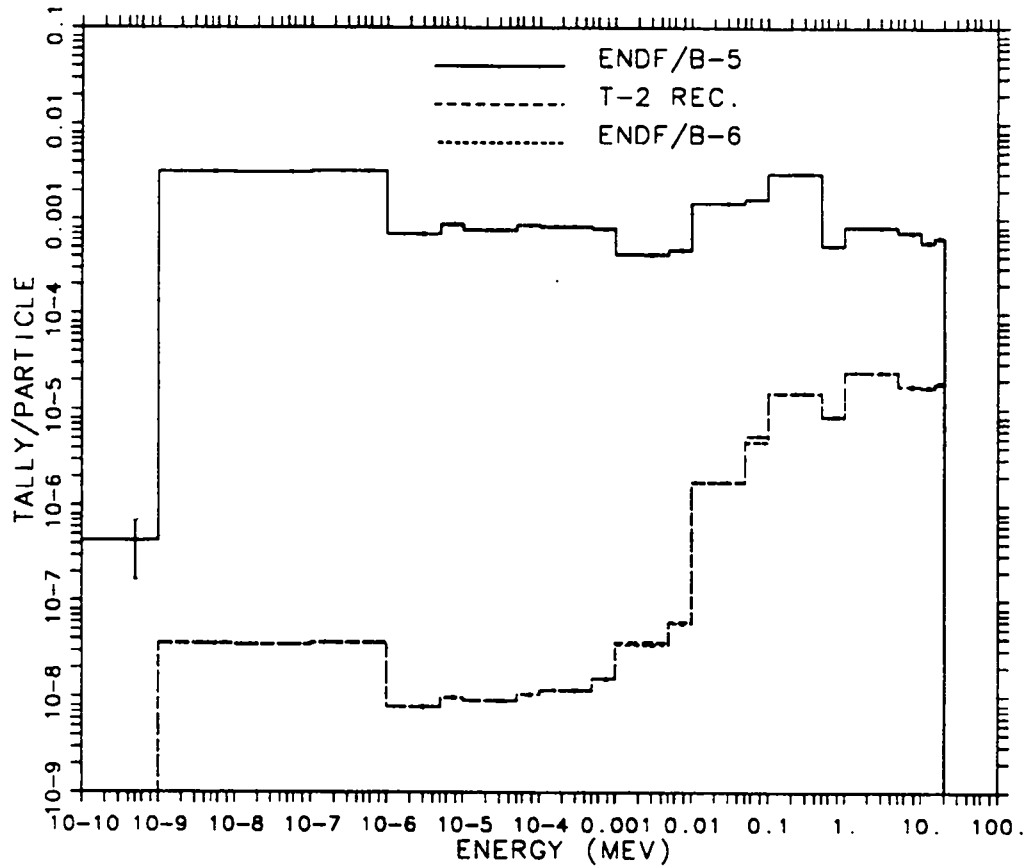


Figure 7: Plot of ENDF/B-V, MCNP recommended, and ENDF/B-VI calculated neutron heating for the  $^{197}\text{Au}$  sphere.

## VII. PHOTON PRODUCTION ASSESSMENT

Another part of the validation program was photon production at incident thermal and 14 MeV neutron energies. Again, these are not comparisons to measured benchmarks, but rather an ENDF/B-V to ENDF/B-VI comparison. These simulations used an isotropic point source inside a thin spherical shell of material. The photon and neutron fluxes were tallied from  $E_\gamma = 0.014$  MeV in 5 keV bins and 20 keV bins respectively.

These results, also to be published,<sup>3</sup> are illustrated in Figures 8-13. For evaluations which were translated from ENDF/B-V, the photon production assessment showed no differences between the two data libraries as shown for Si in Figures 8 and 9. For new evaluations, there were often substantial changes for photon production at both thermal and 14-MeV incident neutron energies. In general, photon production is represented by discrete energy gamma-ray lines, wide histogram energy bins, or a combination of the two. The new ORNL evaluations generally use histogram energy bins for photon production from thermal neutrons, while usually using a combination of the two for photon production from 14-MeV neutrons.

The comparisons for photon production from Cr, using the new ORNL evaluations, are illustrated in Figures 10 and 11. The energy resolution for photon production at thermal energies has been improved from 250 keV to 100 keV. The energy resolution for photon production at 14 MeV shows substantial improvement; however, the combination of discrete photon energies with histogram energy bins may make spectral analysis difficult for some applications. The new evaluations were verified by hand checking to be properly represented. The comparisons for photon production from F are illustrated in Figures 12 and 13. The energy resolution for photon production at thermal energies has been substantially decreased, thereby losing the majority of the discrete photons that are present in the ENDF/B-V libraries. The reverse is true for photon production at 14 MeV from F.

Substantial improvements in energy resolution have been made in the ENDF/B-VI evaluations, though the combination of histogram and discrete energy photon representations may make spectral analysis difficult as for Cr. The recommended ENDF library to use for applications requiring detailed photon production treatment will therefore be dependent upon the neutron energy range of interest and the specific requirements of the application.

## VIII. LIVERMORE PULSED SPHERE BENCHMARKS

Thirty-eight neutron pulsed sphere experiments were performed at Lawrence Livermore National Laboratory in the late 1960's to evaluate the performance of several neutron transport codes.<sup>4</sup> The experiments involved placement of a tritium target in the center of a sphere of a given material. The target was bombarded with deuterium ions to induce the reaction  $T(d,n)^4\text{He}$ , which produces a nearly isotropic source of 14 MeV neutrons. Then the time-of-flight energy spectrum of the neutrons was measured at particular angles. The spheres were

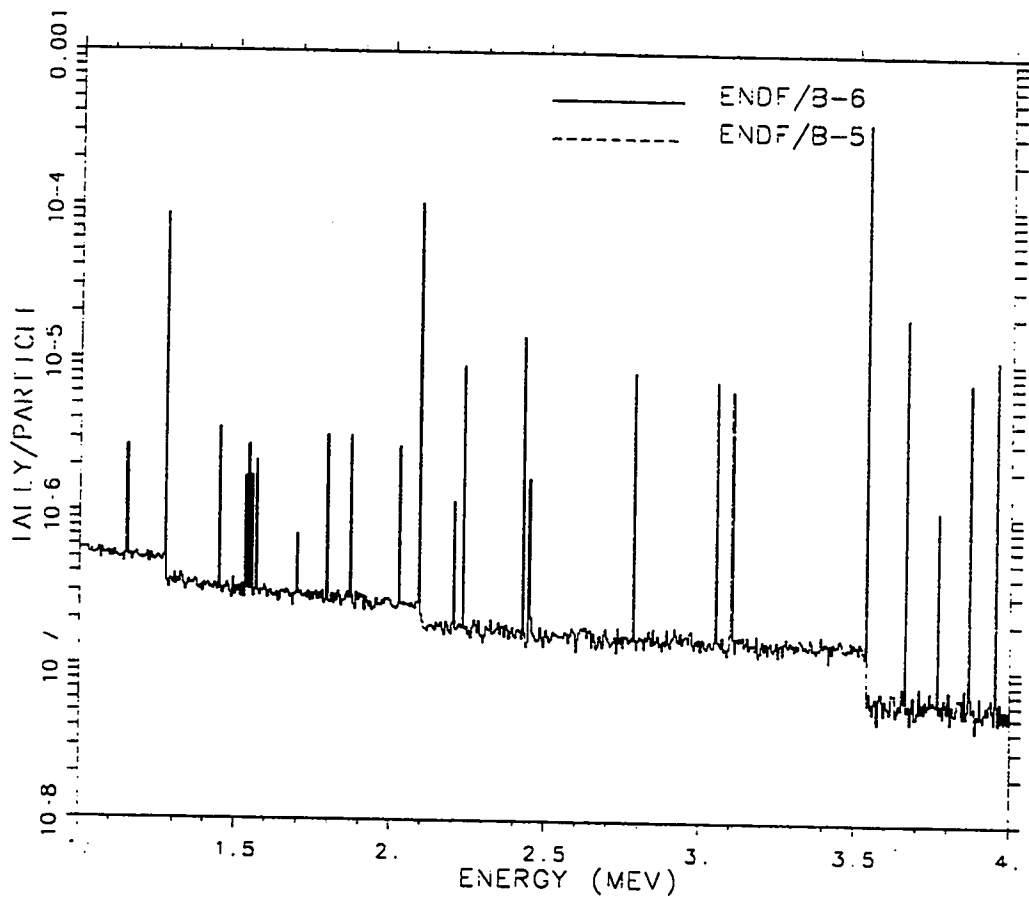


Figure 8: Plot of ENDF/B-V and ENDF/B-VI simulated photon production spectrum from Si at thermal neutron energies.

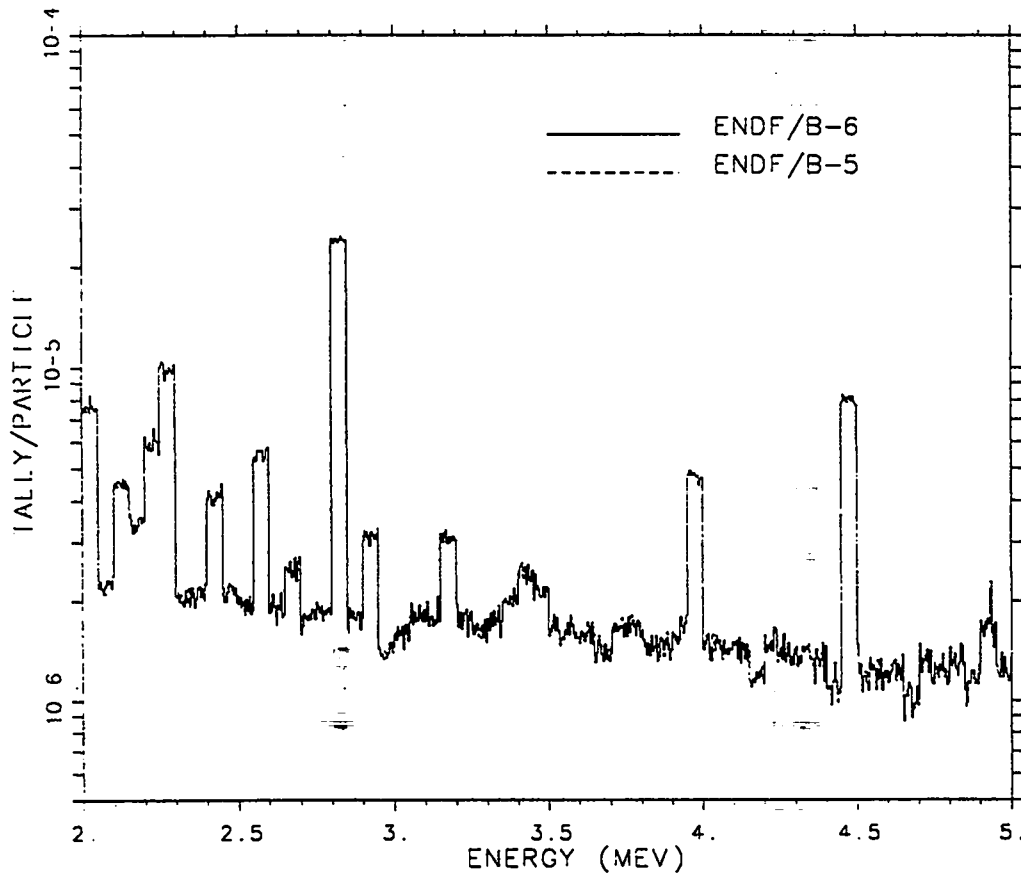


Figure 9: Plot of ENDF/B-V and ENDF/B-VI simulated photon production spectrum from Si for 14 MeV neutrons.

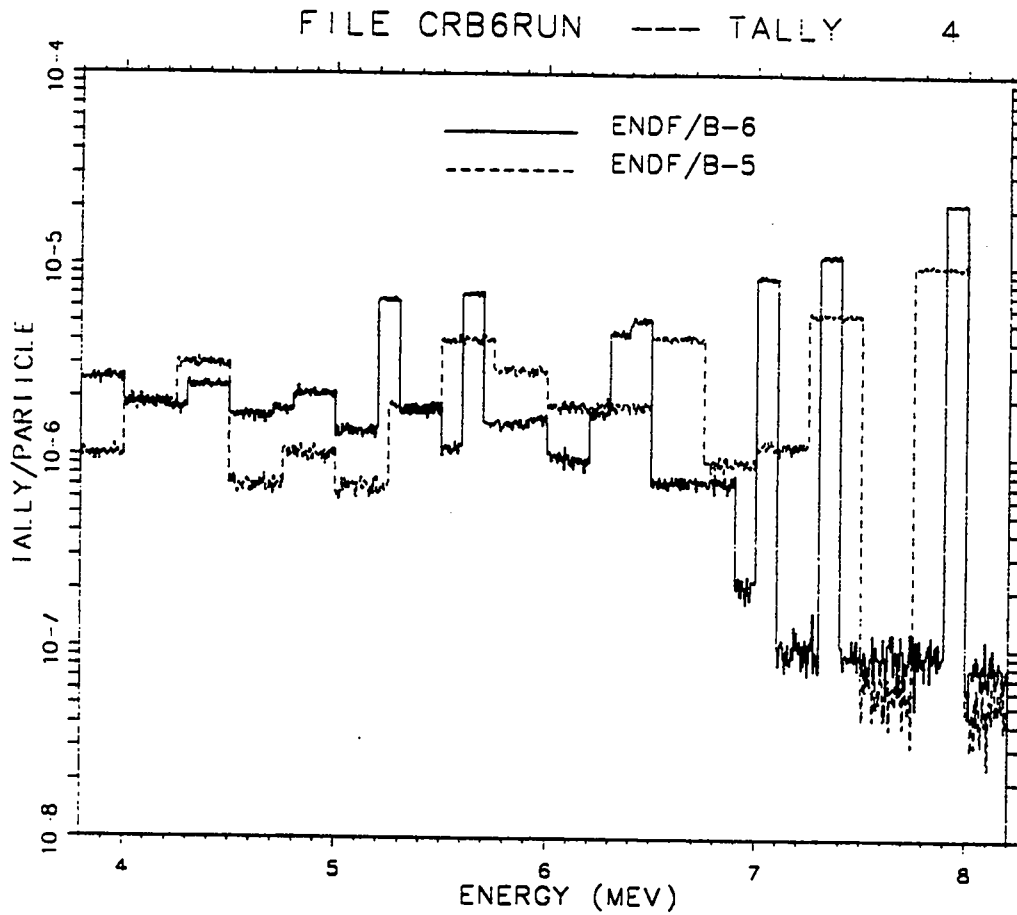


Figure 10: Plot of ENDF/B-V and ENDF/B-VI simulated photon production spectrum from Cr at thermal neutron energies.

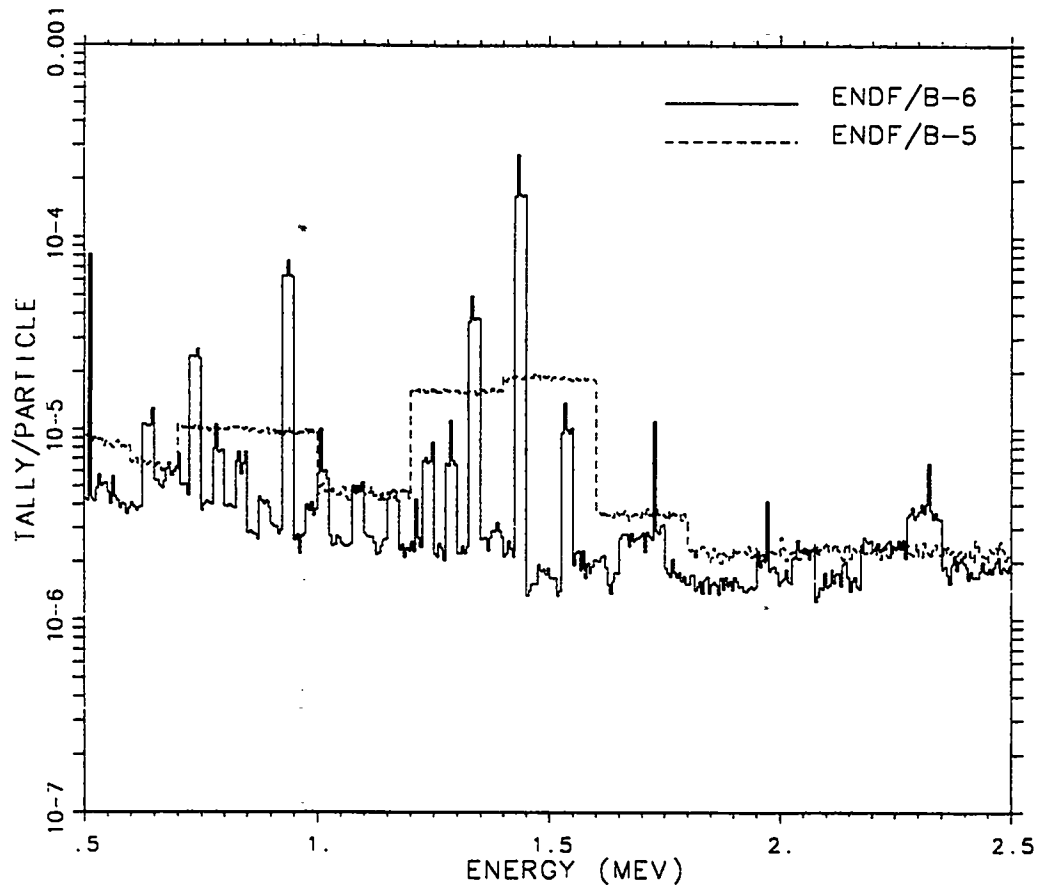


Figure 11: Plot of ENDF/B-V and ENDF/B-VI simulated photon production spectrum from Cr for 14 MeV neutrons.

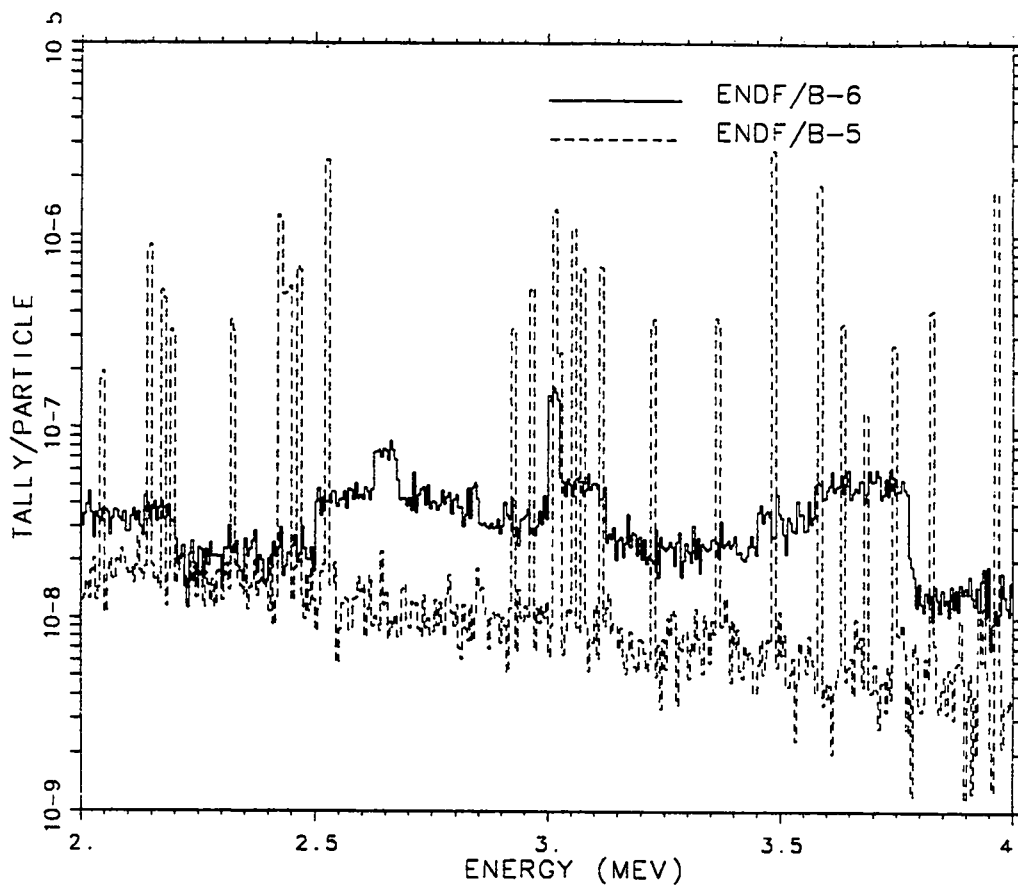


Figure 12: Plot of ENDF/B-V and ENDF/B-VI simulated photon production spectrum from F at thermal neutron energies.

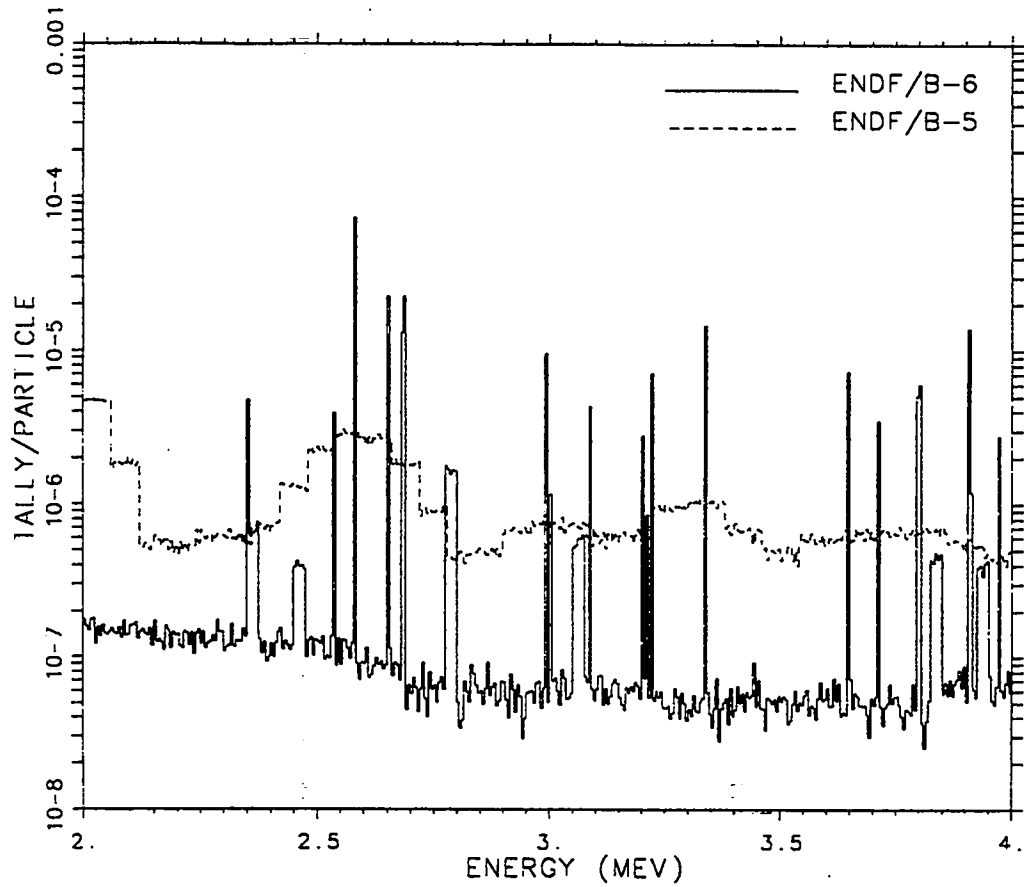


Figure 13: Plot of ENDF/B-V and ENDF/B-VI simulated photon production spectrum from F for 14 MeV neutrons.

from 0.5 to 4.8 mean free paths thick. Twenty-eight of these experimental measurements were simulated with MCNP4A. Table 3 lists the 38 neutron pulsed sphere experiments and indicates which were simulated. In general, when three different thicknesses were measured, only the smallest and largest were simulated. The ratios of calculated-to-experimental results are given in Table 4 for two energy ranges,  $E_n=12.0-16.0$  MeV and  $E_n=2.0-16.0$  MeV, for both ENDF/B-V and ENDF/B-VI.

The results from these calculations<sup>5</sup> differ slightly from the independent preliminary results using MCNP4A with ENDF/B-VI published earlier<sup>6</sup> because we are using the final ENDF60 library rather than a preliminary library and using different assumptions in the problem input, particularly the time-of-flight times to neutron energy correspondence. The data sets were different because in some cases newer revisions of ENDF/B-VI are used in ENDF60, as well as changes between data sets due to modifications in the processing code NJOY. Also, the earlier comparison used some T-2 recommended data, particularly for iron, instead of ENDF/B-V. But in both the preliminary and final studies, the results are consistent.

The ENDF/B-V results more closely represent the experimental results for C and <sup>6</sup>Li as seen in Figures 14-17. However, ENDF/B-V and ENDF/B-VI look about the same in the integral results of Table 4, and we have no evidence from other experiments that C and <sup>6</sup>Li have problems. In particular, ENDF/B-VI results for the CF<sub>2</sub> and CH<sub>2</sub> pulsed spheres were better than ENDF/B-V. The poor results of C and <sup>6</sup>Li in these pulsed sphere experiments may be due to poor experimental measurements or to other materials such as N which was in the air and Fe in the structural material of the experiment.

The ENDF/B-V and ENDF/B-VI results are about the same for O, Mg, Al, Ti, H<sub>2</sub>O, D<sub>2</sub>O, and concrete. The ENDF/B-VI results appear to match the measurements better for <sup>7</sup>Li, Be, N, Fe, Pb, CF<sub>2</sub> and CH<sub>2</sub>. The results for N are plotted in Figures 18-19. The T-2 recommended library for Fe appears better than either ENDF/B-V or ENDF/B-VI.

## IX. IRON BENCHMARKS

The ENDF/B-VI isotopic iron cross section data were subjected to four benchmark studies as part of the Hiroshima/Nagasaki dose re-evaluation for the National Academy of Sciences and the Defense Nuclear Agency.<sup>7</sup> The four benchmark studies were (1) the iron sphere benchmarks from the Lawrence Livermore Pulsed Spheres which are repeated from the above study; (2) the ORNL Fusion Reactor Shielding Benchmark; (3) a 76-cm diameter iron sphere benchmark done at the University of Illinois; and (4) the ORNL Benchmark for Neutron Transport through Iron which used a fission reactor source. In all cases, the ENDF60 library was compared to the ENDF/B-V and T-2 recommended data libraries. Although experimental data were available for all four benchmarks, the description of the experimental setup and interpretation of the experimental results were inadequate in two cases to obtain reasonable agreement between measurements and either ENDF/B-V or ENDF/B-VI. But for the Hiroshima/Nagasaki dose re-

Table 3: Livermore Pulsed Spheres Target Material Outline.

Material	Radius (mfp)	Used for ENDF/B-VI
<sup>6</sup> Li	0.5	✓
	1.1	
	1.6	✓
<sup>7</sup> Li	0.5	✓
	1.0	
	1.6	✓
Beryllium	0.8	✓
Carbon	0.5	✓
	1.3	
	2.9	✓
Nitrogen	1.1	✓
	3.1	✓
Oxygen	0.7	✓
Magnesium	0.7	✓
	1.2	
	1.9	✓
Aluminum	0.9	✓
	1.6	
	2.6	✓
Titanium	1.2	✓
	2.2	
	3.5	✓
Iron	0.9	✓
	2.9	
	4.8	✓
Lead	1.4	✓
H <sub>2</sub> O	1.1	✓
	1.9	✓

Table 3 (cont.) Livermore Pulsed Spheres Target Material Outline.

Material	Radius (mfp)	Used for ENDF/B-VI
D <sub>2</sub> O	1.2	✓
	2.1	✓
CH <sub>2</sub>	0.7	✓
	1.6	
	3.0	✓
CF <sub>2</sub>	0.9	✓
	1.8	
	2.9	✓
Concrete	2.0	✓
	3.8	

Table 4: Ratio of Calculated to Experimental Results for the Livermore Pulsed Spheres.

Material	Radius (mfp)	Energy Range (MeV)	ENDF/B-V	MCNP Rec.	ENDF/B-VI
<sup>6</sup> Li	0.5	12-16	0.980	0.982	0.951
		2-16	0.986	0.987	0.984
	1.6	12-16	1.022	1.028	0.929
		2-16	1.037	1.041	0.997
<sup>7</sup> Li	0.5	12-16	0.961	0.992	0.993
		2-16	0.983	0.990	0.989
	1.6	12-16	0.940	1.036	1.032
		2-16	1.003	1.027	1.018
Beryllium	0.8	12-16	0.936	*	0.962
		2-16	1.000	*	0.988
Carbon	0.5	12-16	0.974	*	0.995
		2-16	0.994	*	1.022
	2.9	12-16	0.942	*	1.017
		2-16	0.971	*	1.066
Nitrogen	1.1	12-16	0.903	0.903	0.952
		2-16	0.965	0.965	0.988
	3.1	12-16	0.849	0.851	0.938
		2-16	0.982	0.983	1.017
Oxygen	0.7	12-16	0.934	0.934	0.927
		2-16	0.996	0.996	0.990
Magnesium	0.7	12-16	1.044	*	1.045
		2-16	1.033	*	1.032
	1.9	12-16	0.997	*	0.998
		2-16	0.965	*	0.965
Aluminum	0.9	12-16	0.939	*	0.939
		2-16	0.947	*	0.947
	2.6	12-16	0.794	*	0.796
		2-16	0.843	*	0.843

<sup>a</sup>Energy range corresponds to 16 Shakes or less for all materials except concrete, which corresponds to 20.5 Shakes or less.

<sup>b</sup>Energy range corresponds to 35 Shakes or less for all materials except concrete, which corresponds to 47.7 Shakes or less.

\*No T-2 evaluations were contained in these materials.

Table 4 (cont.) Ratio of Calculated to Experimental Results for the Livermore Pulsed Spheres.

Material	Radius (mfp)	Energy Range (MeV)	ENDF/B-V	MCNP Rec.	ENDF/B-VI
Titanium	1.2	12-16	1.060	*	1.063
		2-16	0.988	*	0.988
	3.5	12-16	1.088	*	1.088
		2-16	0.945	*	0.943
Iron	0.9	12-16	0.989	1.001	0.999
		2-16	0.984	1.007	1.006
	4.8	12-16	0.866	0.934	0.903
		2-16	0.834	0.946	0.952
Lead	1.4	12-16	0.883	0.883	0.885
		2-16	0.861	0.860	0.911
Water H <sub>2</sub> O	1.1	12-16	0.897	0.898	0.891
		2-16	0.955	0.995	0.947
	1.9	12-16	1.015	1.014	1.005
		2-16	1.074	1.073	1.062
Heavy Water D <sub>2</sub> O	1.2	12-16	0.875	0.875	0.868
		2-16	0.927	0.922	0.912
	2.1	12-16	1.015	0.986	0.975
		2-16	1.029	1.024	1.012
Polyethylene CH <sub>2</sub>	0.7	12-16	0.973	*	0.991
		2-16	1.002	*	1.020
	3.0	12-16	0.898	*	0.953
		2-16	0.988	*	1.038
Teflon CF <sub>2</sub>	0.9	12-16	0.962	*	1.027
		2-16	0.978	*	1.045
	2.9	12-16	0.754	*	0.920
		2-16	0.778	*	0.942
Concrete	2.0	12-16	1.004	1.004	0.999
		2-16	1.052	1.052	1.042

<sup>a</sup>Energy range corresponds to 16 Shakes or less for all materials except concrete, which corresponds to 20.5 Shakes or less.

<sup>b</sup>Energy range corresponds to 35 Shakes or less for all materials except concrete, which corresponds to 47.7 Shakes or less.

\*No T-2 evaluations were contained in these materials.

CARBON (0.5 M. F. P.)

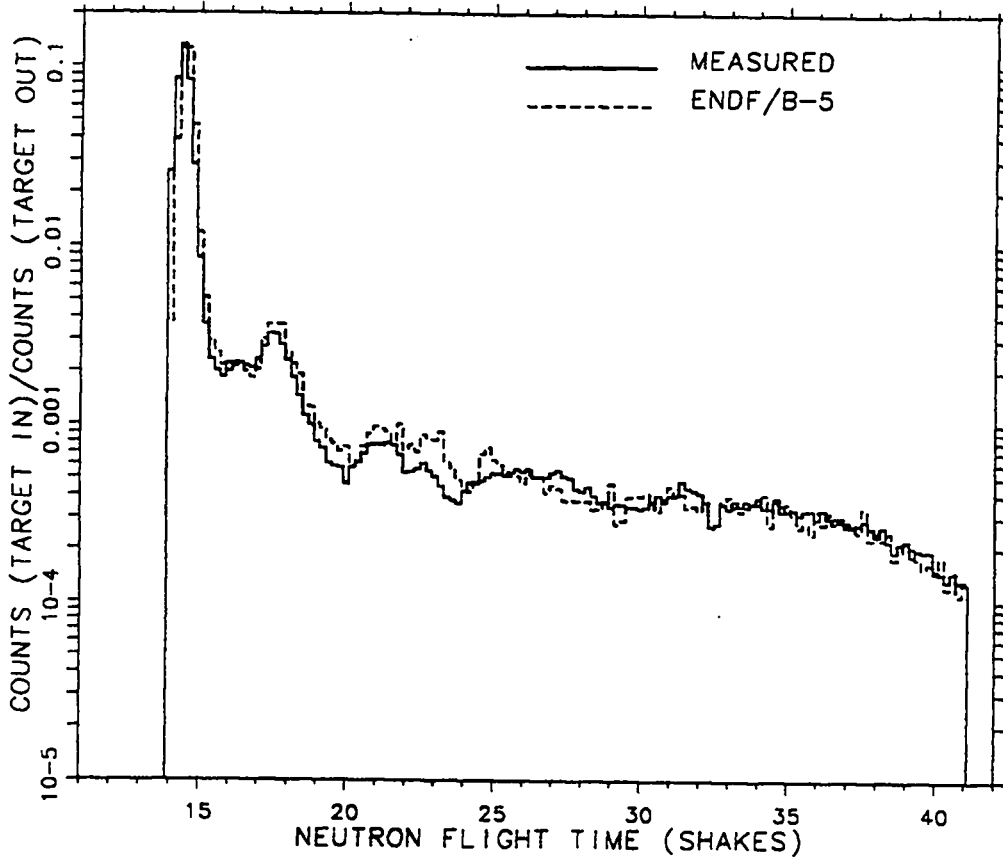


Figure 14: Plot of experimental and ENDF/B-V calculated count rates for the carbon sphere of 0.5 mean free path radius.

CARBON (0.5 M. F. P.)

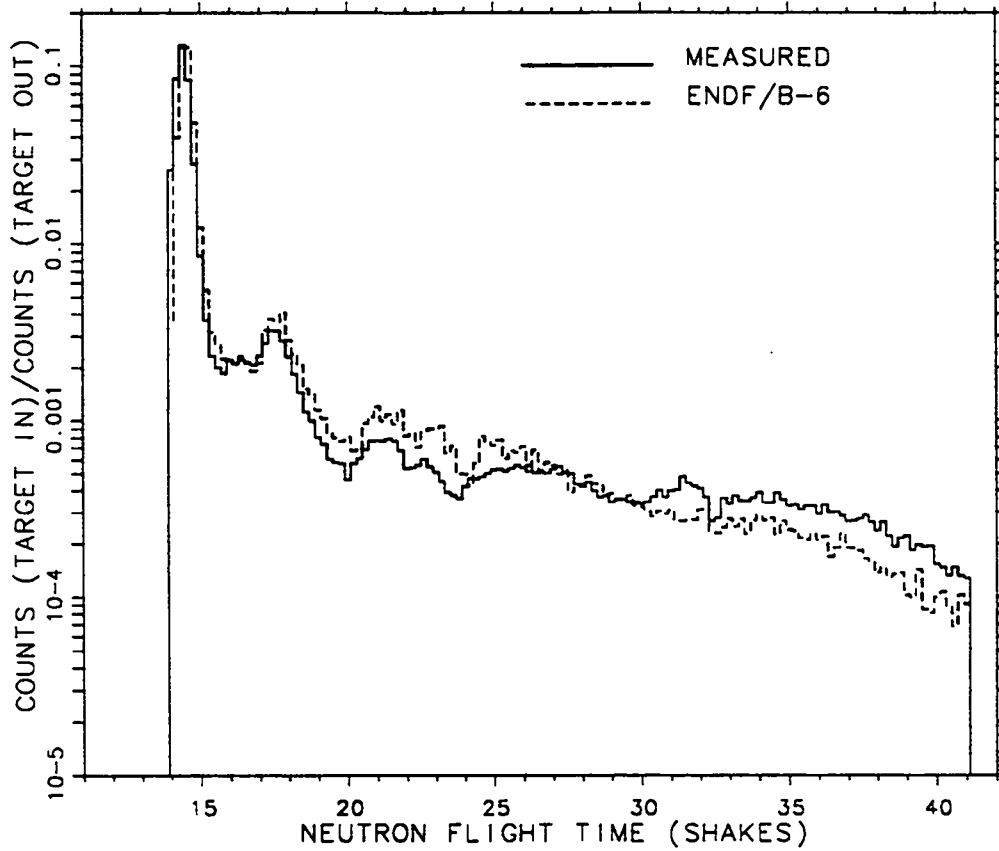


Figure 15: Plot of experimental and ENDF/B-VI calculated count rates for the carbon sphere of 0.5 mean free path radius.

LITHIUM-6 (0.5 M. F. P.)

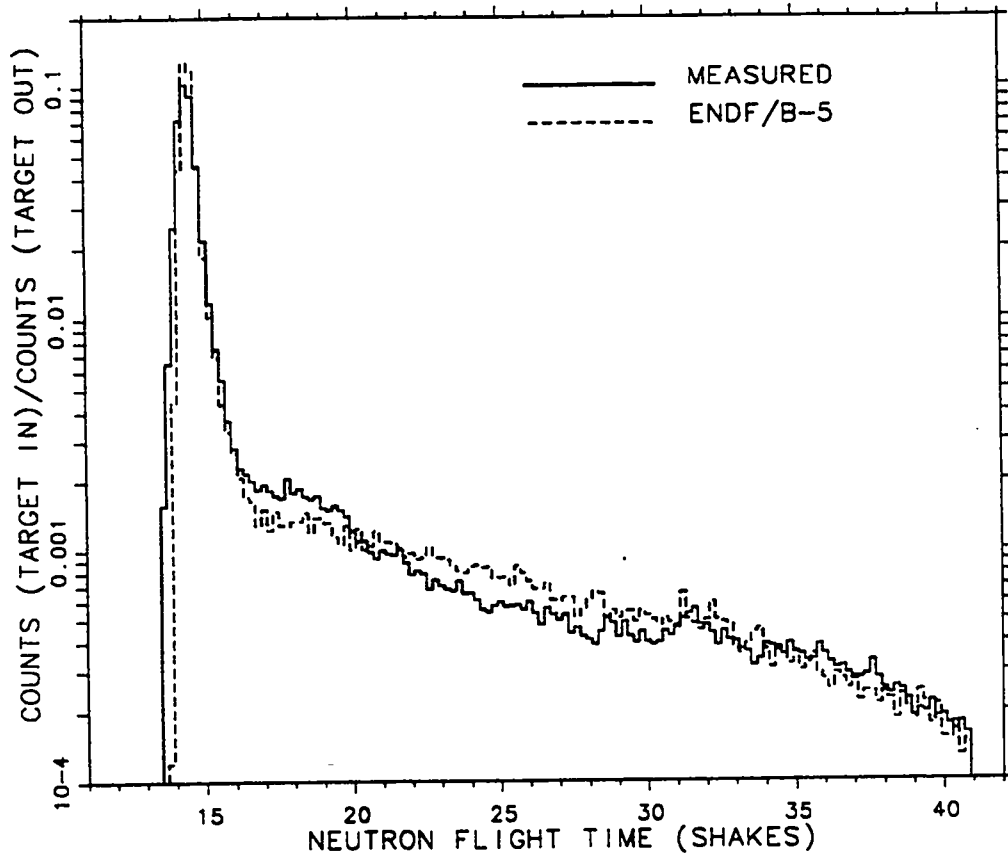


Figure 16: Plot of experimental and ENDF/B-V calculated count rates for the <sup>6</sup>Li sphere of 0.5 mean free path radius.

LITHIUM-6 (0.5 M. F. P.)

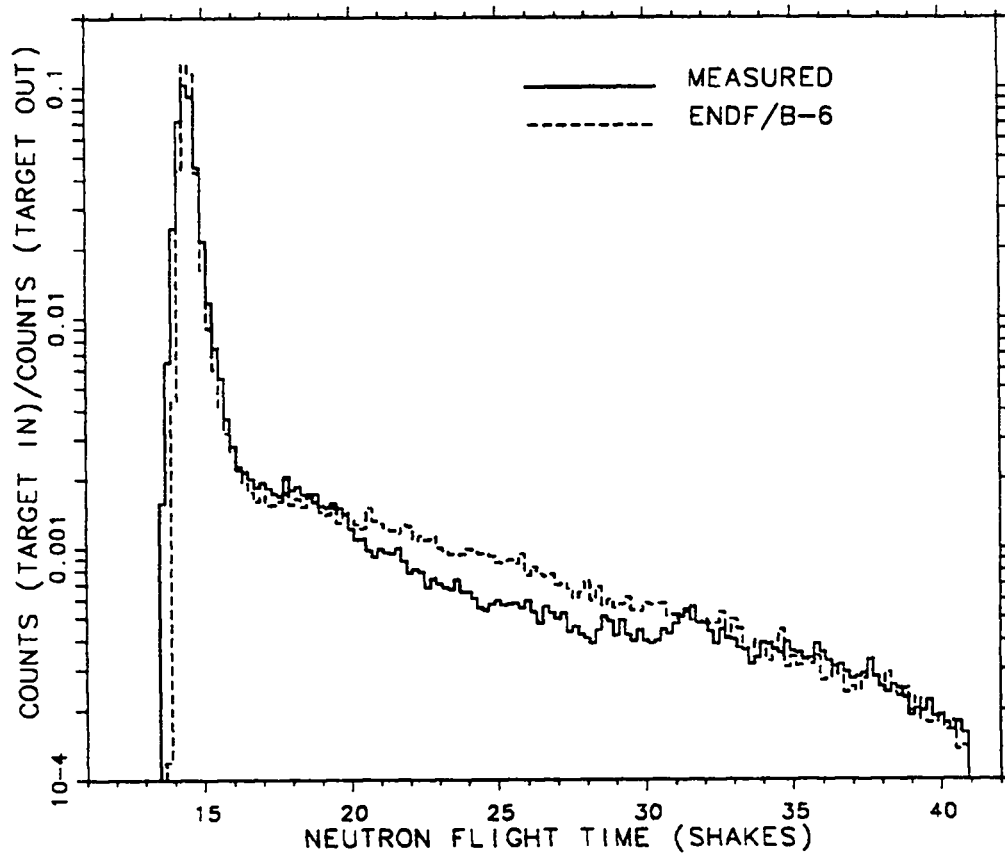


Figure 17: Plot of experimental and ENDF/B-VI calculated count rates for the <sup>6</sup>Li sphere of 0.5 mean free path radius.

NITROGEN (3.1 M. F. P.)

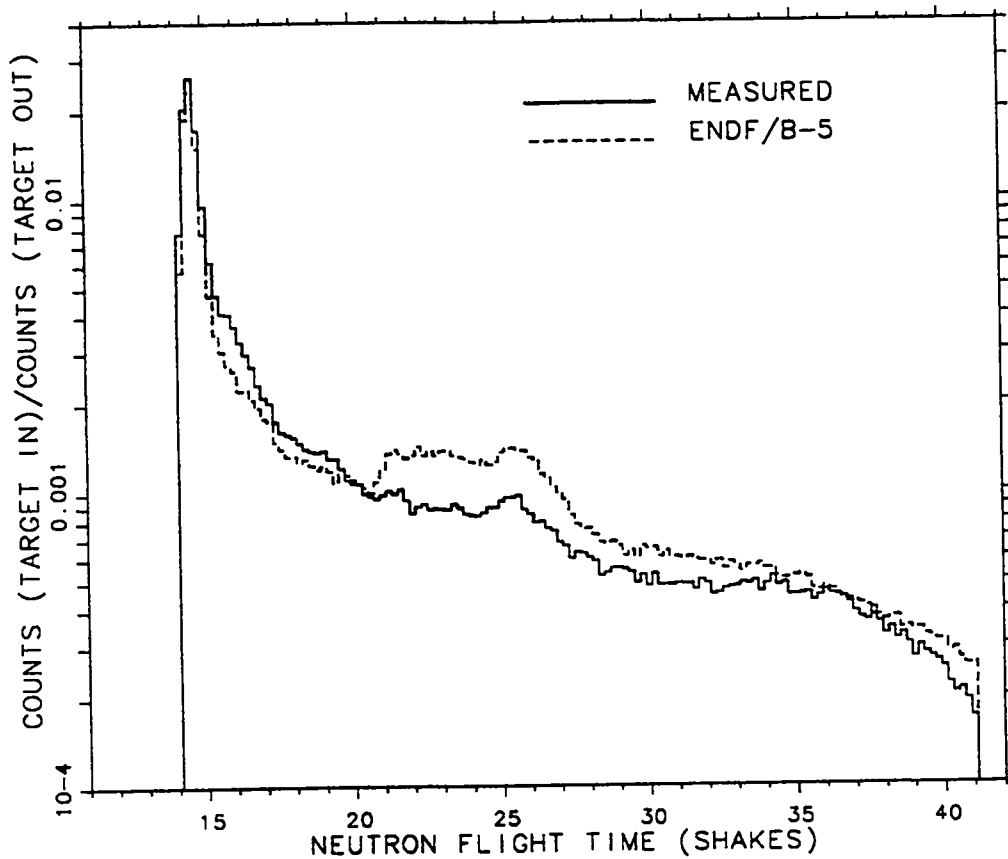


Figure 18: Plot of experimental and ENDF/B-V calculated count rates for the nitrogen sphere of 3.1 mean free path radius.

NITROGEN (3.1 M. F. P.)

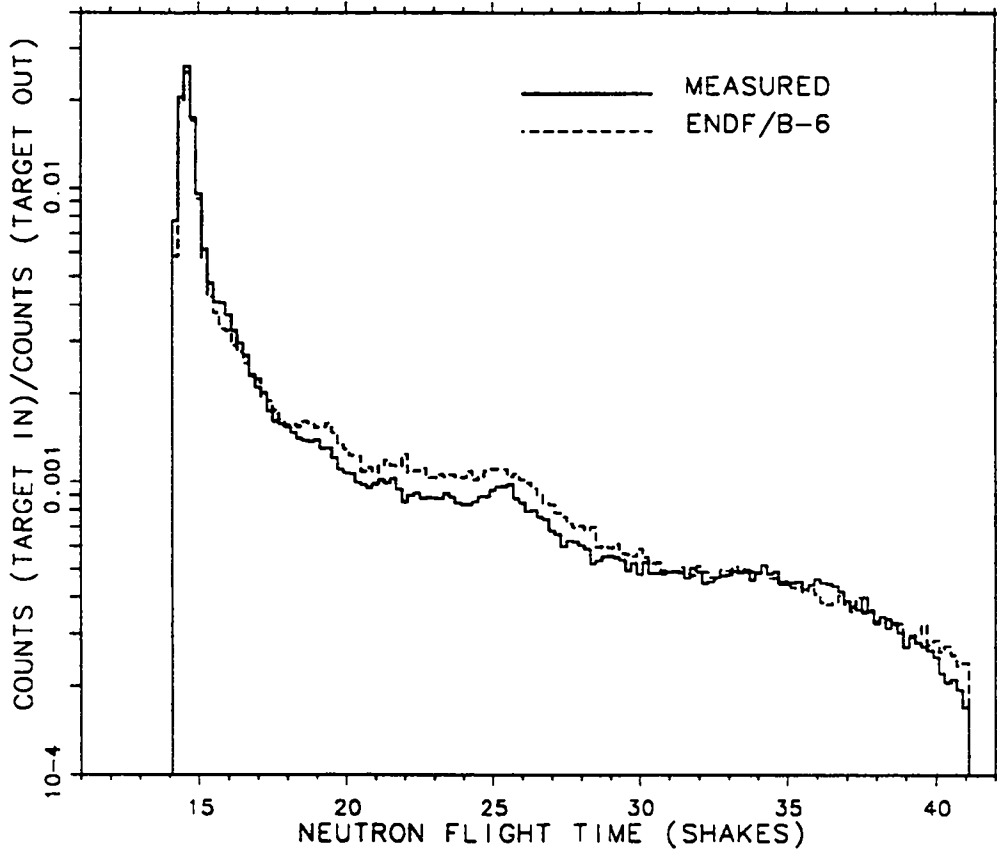


Figure 19: Plot of experimental and ENDF/B-VI calculated count rates for the nitrogen sphere of 3.1 mean free path radius.

evaluation project, the primary purpose was to make a comparison between ENDF/B-VI and ENDF/B-V and the T-2 recommended data libraries.

The Livermore Pulsed Sphere experiments have already been described.

Oak Ridge National Laboratory Fusion Reactor Shielding Benchmark was undertaken to simulate the radiation exposure that would be present at the first wall of a fusion reactor. Again, the  $T(d,n)^4\text{He}$  reaction was utilized by bombarding a tritiated target with a deuteron beam, resulting in a nearly-isotropic source of 14 MeV neutrons. The tritiated titanium target was imbedded inside an iron cavity liner which served as a spectrum modifier and made the neutron spectrum incident on the experimental shield configuration similar to the spectrum incident on the first wall of a fusion reactor. The 14 MeV neutrons passed through several different configurations of laminated slabs composed of SS-304 and borated polyethylene. Four configurations were modeled: configurations 1, 2, 3, and 7. Table 5 shows the shielding configuration compositions. Table 6 shows the ratio of calculated to experimental flux transmissions for the two detector positions, on and off axis, and for the 5 neutron energy regions,  $E_n=0-2, 2-5, 5-10, 10-13,$  and  $>13$  MeV. Generally ENDF/B-VI and the T-2 MCNP recommended iron cross sections agree and give larger flux transmissions than the ENDF/B-V data. A comparison of the calculated to experimental results shows that agreement is best for the T-2 recommended library 18 times, the ENDF/B-VI library 12 times, and the ENDF/B-V library only 7 times. The experimental data are given in the form of experimental upper and lower bounds. In Figures 20 and 21, the results for the thickest shielding are shown. ENDF/B-VI agrees much more closely to the experiment than ENDF/B-V for configuration 7.

The University of Illinois conducted neutron leakage experiments on a 76-cm-diameter iron sphere in the early 1970's. The sphere contained a 15-cm void in the center, where two types of sources were used in the measurements: 14 MeV neutrons from the  $T(d,n)^4\text{He}$  reaction and a  $^{252}\text{Cf}$  source. Comparisons were made between ENDF/B-VI and ENDF/B-IV, ENDF/B-V, and the T-2 recommended library. Comparisons to experimental results are not presented because the description of the experimental setup and results was insufficient to obtain reasonable agreement. The results are detailed in Table 7 and show that the ENDF/B-VI and T-2 recommended libraries are in good agreement, while the ENDF/B-IV and ENDF/B-V libraries tend to show reduced flux transmission,

The ORNL Benchmark for Neutron Transport through Iron used a highly collimated beam of fission-spectrum neutrons that was nearly point mono-directional on 4 thicknesses of iron. The flux at various angles and distances from the back face of the iron slab was measured with three types of detectors. The results of the simulations are presented in Tables 8-11. The percentage deviations from experiment indicate that our model is not an accurate representation of the experimental setup. Nevertheless, the results are useful in that they again demonstrate that the T-2 recommended library is generally close to the ENDF/B-VI iron in results, and that both



Table 6: Fusion Reactor Shielding Integrated Energy Group Comparisons

Configuration	Detector Position	Energy Group (MeV)	ENDF/B-V	T-2 Rec.	ENDF/B-VI
1	On	0-2	1.249	1.157	1.164
		2-5	1.140	1.143	1.140
		5-10	1.000	1.000	1.000
		10-13	0.934	0.955	1.109
		> 13	1.116	1.100	0.949
2	On	0-2	1.003	0.997	0.982
		2-5	0.981	1.000	1.012
		5-10	0.865	1.000	1.000
		10-13	1.000	1.056	1.054
		> 13	1.035	1.085	1.043
3	On	0-2	0.979	1.000	0.970
		2-5	0.875	0.999	1.000
		5-10	0.770	0.970	1.000
		10-13	0.949	1.000	1.000
		> 13	0.953	1.039	0.972
	Off	0-2	1.258	1.301	1.255
		2-5	1.000	1.145	1.127
		5-10	0.869	1.000	1.018
		10-13	0.910	1.000	1.000
		> 13	1.170	1.356	1.217
7	On	0-2	0.798	0.901	0.842
		2-5	0.823	0.997	0.961
		5-10	0.848	1.000	1.000
		10-13	0.910	1.000	1.000
		> 13	1.000	1.097	1.038
	Off	0-2	0.736	0.822	0.793
		2-5	0.757	0.948	0.921
		5-10	0.765	0.951	1.000
		10-13	0.870	1.000	1.000
		> 13	0.907	1.016	0.977

CONFIGURATION 7 - ON AXIS  
ENDF/B-5

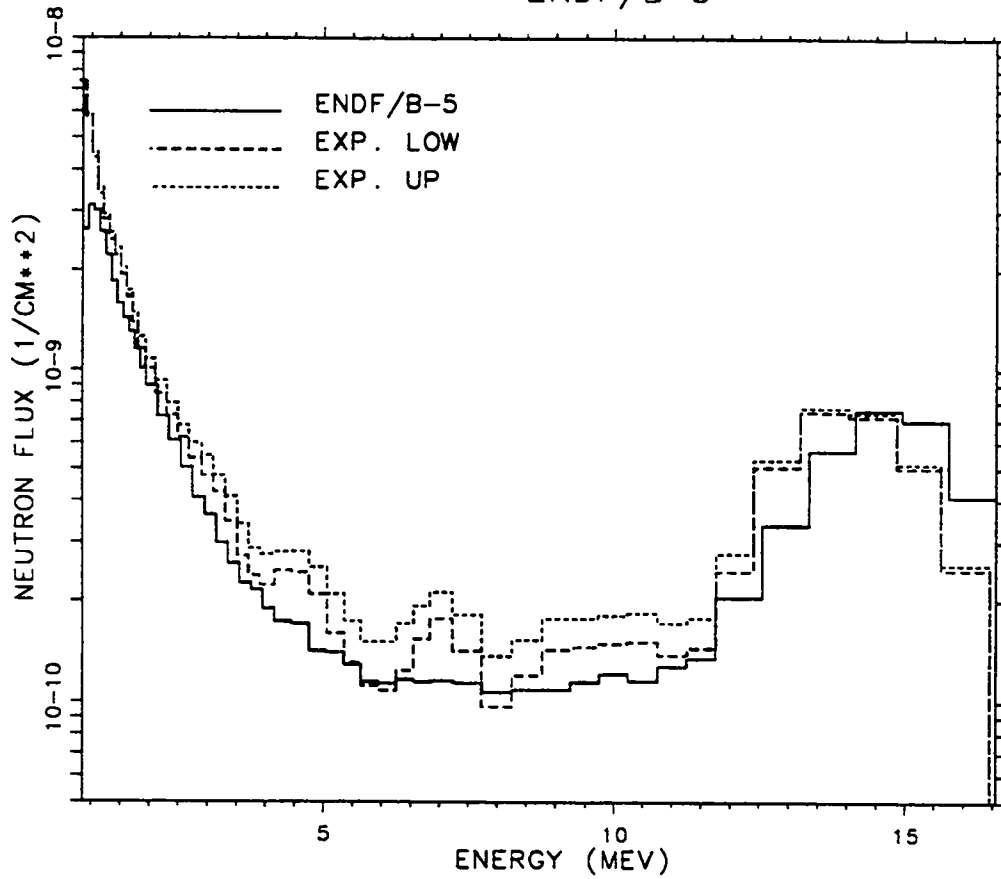


Figure 20: Plot of ENDF/B-V calculated and experimental upper and lower confidence levels for configuration 7 with the detector on axis.

CONFIGURATION 7 - ON AXIS  
ENDF/B-6

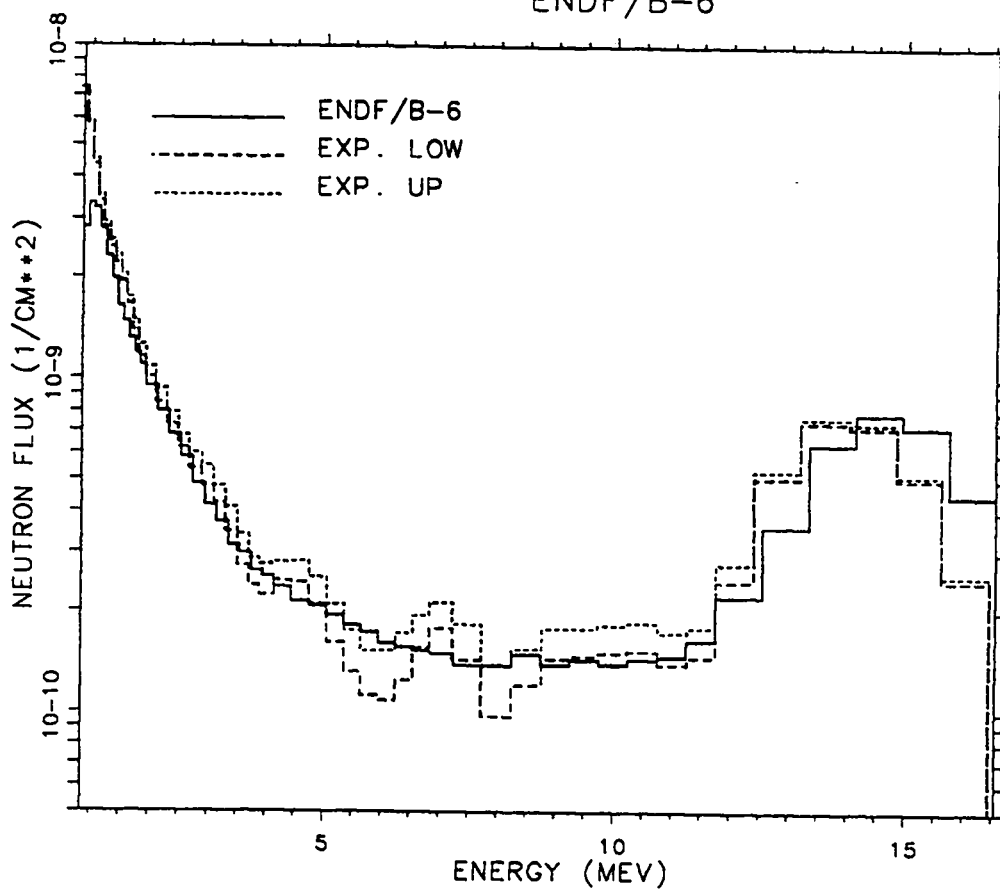


Figure 21: Plot of ENDF/B-VI calculated and experimental upper and lower confidence levels for configuration 7 with the detector on axis.

Table 7: 76 cm. Iron Sphere Results: ENDF/B-VI Data Set Differences

Composition	Source	Energy Group (MeV)	% Difference $(\frac{ENDF/B-VI-ENDF/B-z}{ENDF/B-z}) \times 100$		
			ENDF/B-IV	ENDF/B-V	T-2 Rec.
Pure Iron	$^{252}\text{Cf}$	0.5-2	+4.54	+0.342	-2.02
		2-5	+17.48	+14.11	+1.739
		5-10	+21.0	+22.8	+10.48
		10-13	+82.2	+128.2	+16.5
		> 13	+41.6	-56.8	-21.6
	T(d,n) $^4\text{He}$	0.5-2	+0.819	+1.017	-2.76
		2-5	+20.8	+19.22	-1.580
		5-10	+36.9	+39.2	+14.44
		10-13	+12.62	+11.93	-0.769
		> 13	+2.33	+3.32	-10.81
High Carbon Steel	$^{252}\text{Cf}$	0.5-2	*	+3.21	-0.723
		2-5	*	+11.11	+2.91
		5-10	*	+18.22	+19.48
		10-13	*	-17.72	-31.9
		> 13	*	-16.95	-1.211
	T(d,n) $^4\text{He}$	0.5-2	*	+2.53	-0.802
		2-5	*	+21.8	+1.913
		5-10	*	+43.3	+15.05
		10-13	*	+19.07	+2.86
		> 13	*	+5.22	-8.22
*Contains isotopes not available in ENDF/B-IV					

Table 8: Comparison to Experiment for the 3.94 cm Iron Slab.

Data Set	Observation Angle (deg)	% Deviation from Experiment		
		3.09 inch	5.88 inch	9.86 inch
ENDF/B-IV	0	2.0	-3.3	0.1
	15	10.3	0.9	-0.3
	45	10.9	8.0	7.5
ENDF/B-V	0	1.7	-4.4	-0.7
	15	10.1	1.1	0.3
	45	9.7	7.6	8.0
T-2 Rec.	0	2.4	-3.2	0.1
	15	9.5	0.8	1.1
	45	8.9	6.6	8.0
ENDF/B-VI	0	2.4	-2.5	0.6
	15	10.7	0.8	1.6
	45	10.4	6.3	7.9

Table 9: Comparison to Experiment for the 30.81 cm Iron Slab.

Data Set	Observation Angle (deg)	% Deviation from Experiment		
		3.09 inch	5.88 inch	9.86 inch
ENDF/B-IV	0	-4.7	-16.7	-18.5
	15	11.3	6.4	4.3
	45	12.1	10.4	7.5
ENDF/B-V	0	-6.1	-23.5	-28.9
	15	11.0	4.6	0.1
	45	11.4	8.0	2.3
T-2 Rec.	0	-4.6	-17.2	-19.3
	15	9.8	5.6	3.6
	45	10.5	9.3	6.4
ENDF/B-VI	0	1.5	-3.1	-3.1
	15	10.2	5.7	5.3
	45	10.6	9.9	9.2

Table 10: Comparison to Experiment for the 62.00 cm Iron Slab.

Data Set	Observation Angle (deg)	% Deviation from Experiment		
		3.09 inch	5.88 inch	9.86 inch
ENDF/B-IV	0	6.7	-9.3	-18.3
	15	17.8	9.9	-0.1
	45	40.0	27.6	10.6
ENDF/B-V	0	13.6	-6.2	-21.7
	15	20.3	9.4	-5.4
	45	42.9	27.3	5.7
T-2 Rec.	0	10.0	-6.1	-16.4
	15	18.0	9.2	-2.3
	45	38.1	26.1	7.9
ENDF/B-VI	0	16.6	15.4	15.8
	15	12.1	9.6	4.3
	45	32.0	26.9	16.1

Table 11: Comparison to Experiment for the 92.86 cm Iron Slab.

Data Set	Observation Angle (deg)	% Deviation from Experiment		
		3.09 inch	5.88 inch	9.86 inch
ENDF/B-IV	0	18.5	5.2	-7.7
	15	34.2	26.4	8.4
	45	77.4	70.6	47.3
ENDF/B-V	0	31.0	17.9	0.1
	15	40.3	30.7	8.4
	45	81.7	73.5	45.7
T-2 Rec.	0	23.8	11.8	-2.4
	15	35.4	27.3	7.5
	45	77.2	69.4	43.8
ENDF/B-VI	0	28.0	36.9	40.6
	15	29.3	31.0	20.9
	45	81.6	86.1	69.8

allow greater transmission than ENDF/B-V or ENDF/B-IV for iron.

In summary, these 4 sets of iron benchmark calculations showed that when experimental data were available, the T-2 recommended library gave the best agreement, followed by ENDF/B-VI, ENDF/B-V, and ENDF/B-IV. Generally, the T-2 recommended library and ENDF60 tended to agree, whereas the ENDF/B-V and ENDF/B-IV libraries gave lower transmissions. Thus these studies tended to confirm that the T-2 evaluation for iron is still best, followed by ENDF/B-VI, ENDF/B-V, and ENDF/B-IV respectively.

## **X. CRITICALITY BENCHMARKS**

Two sets of criticality calculations were also performed: a set of nine experimental benchmarks for critical assemblies<sup>8</sup> and a set of 25 benchmark problems for KENO code.<sup>9</sup> The calculations were performed using both the ENDF60 and ENDF/B-V libraries. The results for the set of nine experimental benchmarks are shown in Table 12. The second set of tests, the KENO benchmarks, consisted of 25 problems, some of which were repeats of each other and some of which were fictitious, such as an infinite cylinder, and are described in Table 13. The results for the KENO benchmarks are shown in Table 14. Again, the ENDF60 library appears to give results as good as ENDF/B-V or better, thus validating the library. Note that these criticality benchmark results with MCNP4A and the ENDF60 library are not published elsewhere in contrast to the other test problems which are described in greater detail in other reports.

## **XI. DISCUSSION OF THE ENDF60 LIBRARY**

In the process of running the above sets of tests, several problems were encountered, and not all could be corrected. Also, ENDF/B-VI is not always an improvement over ENDF/B-V. Here are the changes to the ENDF60 library required before publicly releasing it and some quirks that still remain in the ENDF60 library.

The <sup>16</sup>O evaluation as processed by NJOY had some cross sections with values less than 10<sup>-37</sup> barns which caused HP workstations to crash. The exponent values were manually increased to 10<sup>-30</sup> in the ENDF60 library.

All new ORNL isotopic evaluations for F, Cr, Mn, Fe, Ni, Cu and Pb used the Legendre polynomial expansion description for energy-angle distributions. Although MCNP does not yet handle this scattering law, these were approximated by NJOY using the Kalbach-87 formalism, with the exception of F. The Kalbach-87 formalism requires scattering in the center-of-mass system but the Legendre expansion representation is in the laboratory system. The NJOY approach to approximating the Legendre expansion with the Kalbach-87 formalism thus set laboratory and center-of-mass energies for the incident neutron to be equal. Therefore energy is

Table 12: Critical Assembly Benchmarks

	ENDF/B-V	T-2	ENDF/B-VI
Godiva 93.71% Enriched Bare Sphere	$1.00008 \pm 0.00104$	*	$0.99525 \pm 0.00108$
Jezebel 95.5% Enriched <sup>239</sup> Pu	$1.01510 \pm 0.00223$	$0.99857 \pm 0.00212$	$1.00228 \pm 0.00217$
Jezebel 80% Enriched <sup>239</sup> Pu	$1.01595 \pm 0.00120$	$1.00799 \pm 0.00121$	$1.00970 \pm 0.00116$
Uranium Cylinder 10.9% Enriched <sup>235</sup> U	$1.00095 \pm 0.00054$	*	$0.99980 \pm 0.00049$
Uranium Cylinder 14.11% Enriched <sup>235</sup> U	$1.00087 \pm 0.00056$	*	$0.99715 \pm 0.00047$
Graphite-Tamped Uranium Sphere	$0.98690 \pm 0.00102$	$0.98850 \pm 0.00110$	$0.98998 \pm 0.00105$
Water-Reflected Uranium Sphere	$0.99667 \pm 0.00190$	*	$0.99606 \pm 0.00191$
Three Cylinders of Uranium Solution	$1.00156 \pm 0.00126$	*	$0.99611 \pm 0.00136$
3 × 3 Array of Plutonium Fuel Rods	$1.00757 \pm 0.00169$	$1.00082 \pm 0.00174$	$0.99916 \pm 0.00154$

Table 13: The KENO Standard Test Set

KENO 1	Simple unreflected $2 \times 2 \times 2$ array of 93.2% enriched uranium metal cylinders.
KENO 2	Identical to KENO 1, with explicit geometry definition.
KENO 3	$2 \times 2 \times 2$ array of 93.2% enriched uranium metal cylinders reflected by 15.24 cm of paraffin on all six sides.
KENO 4	Identical to KENO 3 with different paraffin specifications.
KENO 5	Identical to KENO 3 and 4 except with 30.48 cm of paraffin.
KENO 6	Single unreflected uranium cylinder from KENO 1.
KENO 7	Identical to KENO 1 and 2 but using specular reflection.
KENO 8	Infinitely long uranium cylinder using the materials and radius of KENO 1.
KENO 9	Infinite array of KENO 1 units through the use of specular reflection.
KENO 10	Identical to KENO 1 except set up to write restart information on every fifth cycle.
KENO 11	Restart of KENO 10 from the 50th cycle. (KENO 10 and 11 utilize a KENO feature not needed by MCNP.)
KENO 12	Composite array of 4 93.2% enriched uranium cylinders and 4 Plexiglas containers filled with 92.6% enriched uranyl-nitrite solution.
KENO 13	Two 93.2% enriched uranium cuboids in a uranium metal cylindrical annulus.
KENO 14	One 93.2% enriched uranium cylinder in a uranium metal cylindrical annulus.
KENO 15	Small 97.6% enriched uranium metal sphere supported by a Plexiglass doughnut in a tank of water.
KENO 16	Infinite number of slabs of uranyl-fluoride solution contained in Pyrex glass and separated by borated uranyl-fluoride solution.
KENO 17	Single 93% enriched uranyl-fluoride sphere.
KENO 18	Reflected cubic array of 27 cylinders of aqueous uranyl-nitrate in Plexiglas bottles.
KENO 19	Identical to KENO 12 but using repeated structures.
KENO 20	Critical experiment consisting of seven cylinders in a triangular pitched array.
KENO 21	Critical experiment of an aluminum spherical container, 98% filled with 4.89% enriched uranyl-fluoride.
KENO 22	Identical to KENO 1 using nested holes in a void spacing cuboid.
KENO 23	Identical to KENO 1 using hemi-cylinders.
KENO 24	Identical to KENO 23 but with the hemi-cylinders aligned with the x-axis.
KENO 25	Identical to KENO 23 but with the hemi-cylinders aligned with the y-axis.

Table 14: Keno Benchmarks

	ENDF/B-V	ENDF/B-VI	Change
KENO 1	0.99987 ± 0.00093	0.99365 ± 0.00087	-0.006
KENO 2	0.99987 ± 0.00093	0.99365 ± 0.00087	-0.006
KENO 3	0.99933 ± 0.00112	1.00015 ± 0.00109	+0.001
KENO 4	1.00084 ± 0.00282	0.99983 ± 0.00258	-0.001
KENO 5	1.00042 ± 0.00281	1.00441 ± 0.00293	+0.004
KENO 6	0.74606 ± 0.00074	0.74257 ± 0.00071	-0.003
KENO 7	1.00022 ± 0.00083	0.99536 ± 0.00079	-0.005
KENO 8	0.94036 ± 0.00085	0.93807 ± 0.00070	-0.002
KENO 9	2.29097 ± 0.00100	2.25973 ± 0.00093	-0.031
KENO 10	0.99987 ± 0.00093	0.99365 ± 0.00087	-0.006
KENO 11	0.99987 ± 0.00093	0.99365 ± 0.00087	-0.006
KENO 12	0.99869 ± 0.00121	0.99940 ± 0.00127	+0.001
KENO 13	0.99489 ± 0.00084	0.99141 ± 0.00081	-0.003
KENO 14	0.99849 ± 0.00084	0.99686 ± 0.00082	-0.002
KENO 15	1.00155 ± 0.00097	1.00027 ± 0.00109	-0.001
KENO 16	0.99066 ± 0.00093	0.99235 ± 0.00089	+0.002
KENO 17	1.00290 ± 0.00143	0.99862 ± 0.00152	-0.004
KENO 18	1.02802 ± 0.00126	1.03085 ± 0.00128	+0.003
KENO 19	0.99869 ± 0.00121	0.99940 ± 0.00127	+0.001
KENO 20	0.99707 ± 0.00133	0.99809 ± 0.00147	+0.001
KENO 21	0.99510 ± 0.00082	0.99292 ± 0.00089	-0.002
KENO 22	0.99775 ± 0.00082	0.99551 ± 0.00082	-0.002
KENO 23	0.99987 ± 0.00093	0.99365 ± 0.00087	-0.006
KENO 24	0.99819 ± 0.00081	0.99440 ± 0.00085	-0.004
KENO 25	1.00115 ± 0.00090	0.99516 ± 0.00088	-0.006

not conserved properly. This is a small effect for the heavier elements, but it could have been a significant effect for F.

The original F data as processed by NJOY did not properly sample both spectra given in the evaluation for the (n,2n) reaction. Thus the original F data was replaced with one in which the (n,2n) reaction was broken into two reactions, MT=6 and MT= 46, each with half the true (n,2n) cross section, but one with the first neutron out spectrum and the other with the second neutron-out spectrum. This representation is similar to the treatment in ENDF/B-V of  $^9\text{Be}$ . The correlated energy-angle scattering law (MCNP law 67) is used for approximating the Legendre polynomial expansion description for energy-angle distribution by NJOY, thereby correcting the center-of-mass error found in the other new ORNL evaluations discussed above. A more thorough discussion of these approximations for the Legendre polynomial expansion can be found in the following section.

Another modification to the ENDF/B-VI evaluations using the Kalbach-87 formalism replaces the interpolation scheme for INT=12 with INT=2 for neutrons, but it has been left as INT=12 for photons. However, MCNP treats both neutrons and photons as INT=2 (linear-linear interpolation). This detail is another quirk of the ENDF60 library that should some day be corrected but was left in for the present.

No cadmium file is provided in the ENDF60 library due to an NJOY processing problem. Prior to processing by NJOY, an attempt had been made to add photon production to the ENDF/B-VI Cd (nat) evaluation. This modification of the input data set caused errors with the neutron heating numbers while not fully succeeding at implementing photon production. Since ENDF/B-VI cadmium is simply a translation from ENDF/B-V with no photon production, it was felt that correcting the ENDF/B-VI modified cadmium would cause a significant delay in the release of the ENDF60 library.

The data file cf98249 was also modified to correct an evaluation problem concerning center-of-mass to lab energy conversion. Prior to this correction, neutrons could upscatter above 20 MeV and cause MCNP to crash.

## **XII. APPROXIMATION TO FILE 6, LAW=1, LANG=1**

Several new descriptions for energy and angle distributions of secondary particles from nuclear reactions were implemented in ENDF/B-VI. These were briefly described in Section II. Some of the formats of these new descriptions for file 6 in the ENDF/B-IV evaluations are as follows:

- LCT=1, LAW=1, LANG=1: give angular distributions for each  $E \rightarrow E'$  using Legendre coefficients in the laboratory frame and are used in the ORNL evaluations.
- LCT=2, LAW=1, LANG=2: give angular distributions for each  $E \rightarrow E'$  using Kalbach systematics through the  $R$  parameter in the center-of-mass frame and are used in the LANL and Russian evaluations.

- LCT=1, LAW=7: give secondary energy distributions for a set of emission cosines in the laboratory frame and are used in the LLNL and European Fusion File (EFF) evaluations.
- LCT=2, LAW=6: give distributions in either the laboratory or center-of-mass frame using an analytic law based on phase space and are used in the LANL and Russian evaluations.

There are also two other variations that have not been used which provide for tabulated angular distributions in either the laboratory or center-of-mass frame.

Since MCNP does not yet handle data using LCT=1, LAW=1, LANG=1, it was necessary to approximate the energy-angle distributions using other formalisms. At the time when most of the data for ENDF60 library was processed, NJOY approximated these distributions using the Kalbach-87 formalism, which predicts the following differential cross section in the center-of-mass system,

$$P_{cm}(\mu_{cm}, E, E'_{cm}) = P_{cm}(E, E'_{cm}) \frac{1}{2} \frac{A}{\sinh(A)} [\cosh(A\mu) + R \sinh(A\mu)]. \quad (8)$$

The goal was to select  $P_{cm}(E, E'_{cm})$ ,  $R$ , and  $A$  to obtain reasonable fits to the tabulated laboratory differential cross section given in the ENDF/B-VI evaluations. Unfortunately, full use of this procedure often produces physically unreasonable center-of-mass distributions when applied to the existing data. Therefore, NJOY assumes that the angle-averaged  $P_{cm}$  was identical to  $P_L$ , the  $P_O$  component of the laboratory differential cross section. The forward and backward ratios in the laboratory system,  $P_{L(+1), E, E'}$  to  $P_{cm}(E, E'_{cm})$ , were converted approximately into the corresponding center-of-mass ratios, and the  $R$  and  $A$  parameters were calculated from these ratios where  $R \geq 0$ . The center-of-mass ratios were typically more isotropic than the laboratory ratios. This procedure is easy to implement, but it is not formally correct. It works well for isotropic distributions (low  $E'$  values) and for forward-peaked distributions (high  $E'$  values). It provides a fairly good fit to the forward-scattering energy spectrum and to the backward-scattering spectrum, but the  $P_O$  average could be distorted if the  $R$  value was not close to either 0 or 1. The approximation works better for heavier targets and was used for the Cr, Mn, Fe, Ni, Cu and Pb nuclides of the ORNL evaluations. MCNP samples from the data by using the energy distribution to choose an outgoing energy  $E'$ , and then using the corresponding  $R$  and  $A$  values produced by NJOY to determine an outgoing cosine from the Kalbach formula. A consequence of this approach sets the laboratory and center-of-mass energies for the incident neutron to be equal, thereby not conserving energy.

As was discussed in Sections II and XI, the original F file was replaced due to an error in representing the (n,2n) reaction. When this ORNL evaluation was reprocessed correcting the (n,2n) error, a new approach for approximating LCT=1, LAW=1, LANG=1 had been

implemented in NJOY. Currently, NJOY uses the energy-angle law, with LCT=1 and LAW=7, for approximating the Legendre polynomial expansion version of the energy-angle distributions and was therefore used for F. As this law is already in the laboratory frame, the difficult conversion to the center-of-mass frame is not required, and the energy error found in the other new ORNL evaluations is not present. The first step in this approximation is to choose a set of angle cosines. Inside a loop on incident energy  $E$ , NJOY constructs an outgoing energy spectrum for each of these angles. For use in MCNP, it is also necessary for NJOY to integrate each of the distributions over secondary energy and produce a single-differential distribution  $f(E,\mu)$ . This distribution is then converted into 32 equally probable cosine bins. MCNP samples from this law by using the 32-bin data to select a cosine value.

### **XIII. CONCLUSION**

A standard, "official" MCNP ENDF/B-VI library, the ENDF60 library, is available and has the unique .60C ZAID designator. The ENDF60 library required the development of new scattering laws and sampling techniques in MCNP. It has been tested with infinite media, LLNL Pulsed Sphere benchmarks, photon production tests, critical assembly benchmarks, and iron benchmarks. It is available to MCNP users worldwide so they do not have to generate their own ENDF/B-VI library. Therefore, when they run MCNP with ENDF60, the same library is available for comparison purposes. A new photon library, MCPLIB02, was released with the RSIC package. This new library extends the photon interaction range from 100 MeV to 100 GeV using the LLNL Evaluated Photon Data Library (EPDL). Additionally, the EL1 electron library and an updated XSDIR file were also released. Unlike previous versions, the new XSDIR file defined the default neutron libraries to be the recommended data library as indicated in Appendix G of the MCNP4A manual, and MCPLIB02 as the default photon library.

### **XIV. ACKNOWLEDGMENTS**

The authors gratefully acknowledge the work performed by the Nuclear Theory and Applications Group (T-2) at LANL, and in particular the assistance of R. E. MacFarlane in producing and documenting the ENDF60 data library. The efforts of R. E. Seamon in validating portions of the ENDF60 data library are also gratefully acknowledged. H. Grady Hughes produced and documented the MCPLIB02 photon library.

## XV. REFERENCES

1. Judith F. Briesmeister, Ed., "MCNP4A - A General Monte Carlo N-Particle Transport Code," LA-12625-M, Los Alamos National Laboratory Report, LA-12625-M (1993).
2. J. D. Court, J. S. Hendricks, "MCNP ENDF/B-VI Validation: Infinite Media Comparisons of ENDF/B-VI and ENDF/B-V," Los Alamos National Laboratory Report LA-12887 (December 1994).
3. S. C. Frankle, "Photon Production Assessment for the MCNP Data Libraries," Los Alamos National Laboratory Report, to be published (1995).
4. C. Wong, J. D. Anderson, P. Brown, L. F. Hansen, J. L. Kammerdiener, C. Logan, and B. Pohl, "Livermore Pulsed Sphere Program: Program Summary Through July 1971," Lawrence Livermore National Laboratory Report, UCRL-51144 Rev. 1 (1972).
5. J. D. Court, R. C. Brockhoff, and J. S. Hendricks, "Lawrence Livermore Pulsed Sphere Benchmark Analysis of MCNP ENDF/B-VI," Los Alamos National Laboratory Report, LA-12885 (December 1994).
6. R. C. Brockhoff and J. S. Hendricks, "MCNP Analysis of the Livermore Pulsed Spheres with ENDF/B-VI," Proceedings of the 8th International Conference on Radiation Shielding, American Nuclear Society, Arlington, Texas (April 1994).
7. J. D. Court and J. S. Hendricks, "Benchmark Analysis of MCNP ENDF/B-VI Iron," Los Alamos National Laboratory Report, LA-12884 (December 1994).
8. D. J. Whalen, D. A. Cardon, J. L. Uhle, and J. S. Hendricks, "MCNP: Neutron Benchmark Problems," Los Alamos National Laboratory Report, LA-12212 (November 1991).
9. J. C. Wagner, J. E. Sisolak, G. W. McKinney, "MCNP: Criticality Safety Benchmark Problems," Los Alamos National Laboratory Report, LA-12415 (October 1992).
10. D. E. Cullen, M. H. Chen, J. H. Hubbell, S. T. Perkins, E. F. Plechaty, J. A. Rathkopf, and J. H. Scofield, "Tables and Graphs of Photon-Interaction Cross Sections from 10 eV to 100 GeV derived from the LLNL Evaluated Photon Data Library (EPDL)," Lawrence Livermore National Laboratory report UCRL-50400, Vol. 6 (October 31, 1989).

This report has been reproduced directly from the best available copy.

It is available to DOE and DOE contractors from the Office of Scientific and Technical Information, P.O. Box 62, Oak Ridge, TN 37831. Prices are available from (615) 576-8401.

It is available to the public from the National Technical Information Service, US Department of Commerce, 5285 Port Royal Rd., Springfield, VA 22161.

LOS ALAMOS NAT'L LAB.  
LIB. REPT. COLLECTION  
RECEIVED

'95 JAN 13 PM 6 32

**Los Alamos**  
NATIONAL LABORATORY

Los Alamos, New Mexico 87545